Bachelorthesis

Stephan Hagel

"Properties of light quarks and π-mesons in a moving frame of reference described in Bethe-Salpeter formalism"

German title:

"Eigenschaften leichter Quarks und des π-Mesons in bewegten Bezugsystemen im Bethe-Salpeter Formalismus"

Matrikelnummer: 5007389
Prüfender Dozent: Prof. Dr. Christian Fischer
Zweitprüfer: Prof. Dr. Lorenz von Smekal
Institut: Institut für theoretische Physik

Abstract

In this thesis we will investigate the properties of light quarks and the π-meson (pion) based on the corresponding Dyson-Schwinger equation for quarks and the Bethe-Salpeter equation for bound states of quarks and antiquarks. We investigate, how mass is generated dynamically due to spontaneously broken chiral symmetry in the underlying quantum field theory, quantum chromodynamics (QCD), and we will calculate the effects on the mass and the leptonic decay constant of the pion. Furthermore we will investigate, how these properties behave under Lorentz transformation into a moving frame of reference in our model and what effect different approaches to regularization of the ultraviolet divergence of the theory have.

Zusammenfassung

In dieser Arbeit werden die physikalischen Eigenschaften leichter Quarks und des π-Mesons (Pion) untersucht, indem die zugrunde liegende Dyson-Schwinger Gleichung für Quarks und die Bethe-Salpeter Gleichung für gebundene Quark-Antiquark Zustände gelöst werden. Es wird untersucht, wie Masse durch spontane Symmertriebrüche in der zugrunde liegenden Quantenfeldtheorie (QCD) dynamisch erzeugt wird und wie sich diese Effekte auf die Masse und Zerfallskonstante des Pions auswirkt. Weiterhin wird das Verhalten dieser Eigenschaften unter Lorentz Transformation in ein bewegtes Bezugssystem sowie die Auswirkung verschiedener Regularisierungen auf die Theorie untersucht.

Contents

Chapter 1

Introduction

For a long time humans have been wondering, how the matter that makes up the world is structured. Even ancient Greek philosophers were debating,if everything was a continuous matter made out of the elements fire, water, earth and air (Aristotle, 384 - 322 BC) or if, at the smallest scales, matter was grainy and made out of individual particles that moved freely through empty space (Democritus, c. 460 – c. 370 BC; Leucippus, 5th cent. BC). Certainly, there were no methods back in their days to look even closely at the scales required to confirm either of these models. Because of that, the model of a continuous matter was widely accepted for the longest time, since the idea of completely empty space was hard to comprehend. Only in the early 19th century evidence arose, that matter was made up of elementary particles (Proust, 1799; Dalton, 1805). As time went on, it became clearer and clearer, that these elementary particles exist. In respect to the ancient Greek philosophers, they have been called *atoms*, from the Greek word $\alpha\tau o\mu o\varsigma$ for *irreducible*. It quickly became obvious, that these atoms can't be the final step. Several experiments showed, that an atom has to have an inner structure itself consisting of an electron cloud surrounding a small and massive nucleus. While trying to describe what happens at the scales of the nucleus two main problems arose.

The first one was to combine quantum mechanics, the theory of the smallest scales in the universe, with general relativity, which describes the heaviest and fastest objects. The problem is, that the fundamental equations of quantum mechanics, especially the Schrödinger Equation, are not given in a covariant form, which is required to be compatible with relativity. For the case of special relativity this problem was first solved by P. Dirac, who managed to bring the equation of motion of quantum mechanics into a covariant form, called the Dirac Equation. This let to the discovery of many new physical phenomena, such as spin, negative energies and antiparticles.

The second big problem was the finding, that the nucleus consists of multiple

particles itself which all have a positive electric charge, protons, or have no electric charge at all, neutrons. In the classic model all nuclei containing more than one proton had to be unstable. This lead to the assumption that there is an additional interaction between nucleons that is very strong at small distances but negligible at larger ones. Together with results from deep-inelastic scattering experiments, Gell-Mann and Zweig first proposed a model that explains the spectrum of strongly interacting particles in the early 1960's.Their model describes Mesons and Baryons as bound states of elementary particles, called *quarks*, and their antiparticles. The model needed three different types of quarks, so called flavours, to describe every observed bound state. These flavours are called up (u), down (d) and strange (s).[1] The quarks are spin ½ fermions with an electric charge of +2/3 for up quarks and -1/3 for down and strange quarks. There were still problems with the quark model as it failed to correctly interpret some excited states like the Δ^{++}. It has an electric charge of +2 and spin 3/2 so it has to consist of three up quarks with parallel spin. This would result in a symmetric wave function in spin and flavour space. Since quarks are fermions and obey Fermi-Dirac statistics the wave function of every bound state of quarks has to be antisymmetric. To solve this problem, an additional, unobserved quantum number was proposed – the color. Every quark should have one of three different color charges, red (r), green (g) or blue (b) so that every bound state of quarks and antiquarks should not have any net color. A particle with a symmetric wave function in spin and flavour space can then have a antisymmetric wave function in color space, resulting in a antisymmetric wave function in total.

The quantum field theory describing the strong interaction with the quark model and color charges is known as *Quantum Chromodymanics* (QCD), which we will work with in this thesis. Using fundamental equations of QCD we will see how mass is generated dynamically. While within the standard model the current quark masses are well known, they only make up a small fraction of the hadronic mass. A simple example for this is the proton. It consists of two up and one down quark with a combined current mass of $m_c = 9.0$ MeV,[2] but the proton itself has a mass of $m_p = 928$ MeV [1]. Even for the masses of light mesons a simple addition of the current quark masses is not sufficient anymore. In this thesis the π-meson, or *pion*, is of particular interest, as we will take a closer look at how its mass is generated dynamically in the Bethe-Salpeter formalism. This formalism leads to bound states of quarks and antiquarks which have to satisfy certain conditions by the symmetries of the underlying quantum field theory. For the underlying equation of this formalism, the Bethe-Salpeter equation (BSE), to

[1] As heavier particles have been observed, the model has been extended by the flavours charm (c), bottom (b) and top (t)

[2] Throughout this thesis we will use natural units, see section A.3.

be solved we first need to know the propagator of quarks. It is obtained by solving the Dyson-Schwinger equations (DSE's), a set of self-consistent equations for the quark propagator, the gluon propagator and the quark-gluon vertex including all possible interactions between those. Since the DSE's cannot all be solved in general, some truncation schemes will be applied to give an approximate solution. By solving the BSE we will get information about the pion's fundamental properties, such as its mass and its decay constant. Since these values are Lorentz scalars they should stay invariant under a Lorentz transformation into a moving frame. But since we are applying truncation schemes to simplify the equations, the Lorentz invariance might be violated.

At first this thesis will give a brief introduction to the basic principles that are needed to understand to have the necessary theoretical knowledge. In particular we will take a look at the underlying principles of field theories, especially QCD, and discuss the topic of symmetries and spontaneous symmetry breaking. Then we will introduce the Dyson-Schwinger equation as an equation of motion for the quark propagator as well as the Bethe-Salpeter equation as an equation for bound states of quark-antiquark pairs. We will simplify these equations using the Rainbow-Ladder truncation scheme and take a closer look at multiple ways to regularize the ultraviolet divergence of the theory. After that we investigate the transformation properties of the values obtained in the truncation schemes used and see how the pion's properties behave in a moving frame. The results of this thesis' calculations will then be presented together with the explicit mathematical approach. We will also discuss how far the chosen model is able to reproduce suitable approximations of the experimental values of the physical quantities, which are calculated. Finally, we will reflect the results of the calculations and give an outlook at how the results of this thesis are relevant to present and future research activities.

The appendix includes important conventions and relations that are used often in the calculations of this thesis. Also some important derivations are given explicitly in it.

Chapter 2

Physical principles

2.1 The Lagrangian formalism

In physics it is common that there are multiple ways to solve the same problem. In classical mechanics it does not matter if we use Newton's laws of motion to get the equations of motion of our system or if we use the Lagrangian or Hamilton formalism. The only thing that is important is that the resulting equations have to be equivalent and independent of the formalism used to obtain them. The same thing holds true for quantum field theory. As long as the physics that can be measured stays the same, it is irrelevant how it is described mathematically. So for convenience the Lagrange formalism is used in quantum field theory most of the time. In this formalism our system is described by a Lagrangian density $\mathcal{L}(\phi, \partial_\mu \phi, t)$, which in general depends on the fields ϕ, their derivatives $\partial_\mu \phi$ and the time t. The field equations are obtained in close analogy to classical mechanics by the principle of least action. It states that the physical configurations of the fields are those for which the action

$$S := \int \mathrm{d}^4 x \mathcal{L}(\phi, \partial_\mu \phi, t) \tag{2.1}$$

is stationary, i.e. every variation of it vanishes

$$\delta S|_{\phi=\phi_0} = 0. \tag{2.2}$$

Analogously to classical mechanics one easily derives the Euler-Lagrangian equation

$$\frac{\partial \mathcal{L}}{\partial \phi} = \partial_\mu \frac{\partial \mathcal{L}}{\partial(\partial_\mu \phi)}. \tag{2.3}$$

An example for this is the Lagrangian density of a free spin ½-field, given by

$$\mathcal{L}_0 = \overline{\psi}(i\not{p} - m)\psi, \tag{2.4}$$

where ψ and $\overline{\psi} = \psi^\dagger\gamma_0$ are the operators of the field and its adjoined operator respectively, m is the mass of the particles of the field and p is the momentum operator. We use the Feynman slash notation notation[1]

$$\not{p} = \gamma_\mu p^\mu \tag{2.5}$$

with the gamma matrices γ_μ introduced in section A.2 of the appendix. Plugging this Lagrangian into eq. (2.3) yields

$$(i\not{\partial} - m)\psi = 0 \tag{2.6}$$

$$\overline{\psi}(i\overleftarrow{\not{\partial}} - m) = 0, \tag{2.7}$$

where $\overleftarrow{\not{\partial}}$ implies a differentiation of the field on the left after applying the Feynman slash. Those equations are equivalent to the Dirac equation of free fermions, so the Lagrangian density (2.4) describes this problem correctly.

2.2 Symmetries

In physics, symmetries are of great interest. Not only can they be used to greatly simplify many calculations as it will be seen later on, they also often lead to physical phenomena. One of the great benefits of the Lagrangian formalism is that it is relatively simple to find and interpret symmetries. One important example is Noether's theorem, which states that every differentiable continuous symmetry of a system's Lagrangian density corresponds to a conservation law. One example of such a continuous symmetry is a global phase shift $e^{i\theta}$. Since a wave function cannot be measured itself but its absolute value can, the Lagrangian should be invariant under those phase shifts, i.e.

$$\mathcal{L}(\overline{\psi}, \psi, t) \stackrel{!}{=} \mathcal{L}(\overline{\psi}', \psi', t), \tag{2.8}$$

where $\psi' = e^{i\theta}\psi$ and $\overline{\psi}' = e^{-i\theta}\overline{\psi}$ are the transformed field operator and its adjoined operator. Obviously the free Lagrangian density (2.4) satisfies this condition for

[1]For more information and useful properties of this notation, section A.4 can be consulted.

global phase shifts. Since the set of all global phase shifts is a valid representation of the unitary group of degree 1, we say that the Lagrangian is invariant under transformations of the $U(1)$ group.[2] The conservation law obtained by this symmetry is the continuity equation of classical electrodynamics

$$\partial^\mu j_\mu = \nabla \vec{j} + \frac{\partial \rho}{\partial t} = 0, \tag{2.9}$$

where $j^\mu = (i\rho, \vec{j})$ is the conserved four-vector with ρ being the charge density and $\vec{j}$ being the current density. Integrating eq. (2.9) over all of 3D-Space gives

$$\frac{\partial}{\partial t} \int \mathrm{d}^3 x \rho = \frac{\partial Q}{\partial t} = 0. \tag{2.10}$$

To see that the integral over $\nabla \vec{j}$ is equal to zero, we use Gauss's divergence theorem and use the fact, that $\vec{j}$ has to vanish at infinity. With that we have shown, that invariance under $U(1)$ is equivalent to conservation of electric charge.

Most quantum field theories have additional symmetries. One of them is the generalization of global $U(1)$ invariance to local $U(1)$ invariance, i.e. invariance under all local phase shifts $e^{i\alpha(x)}$. In QCD we get additional degrees of freedom due to the different color charges, which correspond to an $SU(3)$ invariance. From this symmetry several properties of the field theory can be followed. If we take a look at the totally antisymmetric tensor ε_{ijk}, we see that it transforms under an $SU(3)$ transformation according to

$$\varepsilon_{ijk} \to U_{ii'} U_{jj'} U_{kk'} \varepsilon_{i'j'k'} = \det U \varepsilon_{ijk} = \varepsilon_{ijk}, \tag{2.11}$$

since $\det U = 1$. Therefore it is invariant under $SU(3)$. Under the assumption that all hadron wave functions have to be invariant under $SU(3)$ too, it can be shown that the only simple combinations allowed are

$$\overline{q}^i q_i, \quad \varepsilon^{ijk} q_i q_j q_k, \quad \varepsilon_{ijk} \overline{q}^i \overline{q}^j \overline{q}^k, \tag{2.12}$$

which correspond to mesons, baryons and antibaryons respectively.

From the $SU(3)$ invariance additionally follows that new spin 1 particles, the *gluons*, occur, which are the QCD equivalent of the photon. We can also see

[2] In general we say a Lagrangian is invariant under the transformation of a group G, if there is an isomorphic representation $d : G \to GL(V)$ of that group, such that the Lagrangian is invariant under all transformations of the form $\psi \mapsto \psi' = d(A) \cdot \psi$ for all $A \in G$.

that they have to have zero mass, since an additional mass term occurring in the Lagrangian would not be invariant under local $U(1)$ transformations. As a result the full Lagrangian is more complicated than the free Lagrangian (2.4), containing not only the Dirac field ψ, but also gluon terms[2],

$$\mathcal{L} = \overline{\psi}(i\not{D} - m)\psi + \frac{1}{4}F^a_{\mu\nu}F^{\mu\nu}_a, \tag{2.13}$$

where $D^\mu = \partial^\mu + igA^\mu$ is the covariant derivative, $F^{\mu\nu}_a = \partial^\mu A^\nu_a - \partial^\nu A^\mu_a + ig\left[A^\mu_a, A^\nu_a\right]_-$ is the gluon field-strength tensor and A^μ_a, with $a \in (1, 2, \ldots, 8)$, are the eight gluon fields. The full Lagrangian is invariant under local gauge transformations $\psi \to \psi' = U\psi$ with $U(x) \in SU(3)$, if the gluon fields transform according to

$$A^\mu \to (A')^\mu = UA^\mu U^\dagger - \frac{i}{g}U\left(\partial^\mu U^\dagger\right), \tag{2.14}$$

where A^μ_a has been replaced with $A^\mu = A^\mu_a T^a$ and T^a are the generators of the $SU(3)$. If we expand the covariant derivative in the Lagrangian (2.13), we get three different terms $\mathcal{L} = \mathcal{L}_0 + \mathcal{L}_{qg} + \mathcal{L}_{gg}$ The first term $\mathcal{L}_0$ is equal to the free Lagrangian (2.4) and describes the kinetic energy of the Dirac particles. The second term

$$\mathcal{L}_{qg} = -g\overline{\psi}\not{A}\psi \tag{2.15}$$

describes the interaction of quarks and gluons with g being the coupling strength, and lastly the third term

$$\mathcal{L}_{gg} = \frac{1}{4}F^a_{\mu\nu}F^{\mu\nu}_a \tag{2.16}$$

describes the energy density of the gluon fields. In contrast to the Lagrangian of QED, the QCD Lagrangian contains a commutator $[T_a, T_b]_-$ that does not vanish, since $SU(3)$ is a non-Abelian group. Thus the perturbative series of Feynman diagrams also contains three-gluon and four-gluon vertices, fig. 2.1, which we interpret as gluon-gluon interactions. Because of that, the gluons have to carry a color charges themselves in contrast to the photon, which does not carry any charge. This leads to many ways in which a quark can propagate. We will further analyze this when we investigate the quark DSE.

Figure 2.1: The three-gluon and four-gluon vertices arising from the non vanishing commutator $[T_a, T_b]_-$.

2.3 Symmetry breaking

2.3.1 General principles

As already mentioned in the previous section, symmetries are very interesting in physics. It is also interesting to see what happens when symmetries are broken. The phenomenon of the effective quark masses being different from the current quark masses for instance is a consequence of chiral symmetry being spontaneously broken in QCD. To start this section of we first have to define what it means, when a symmetry is *exact*, *broken explicitly* or *broken spontaneously*. [2]

Definition 2.3.1 (Exact symmetry) *Let $\mathcal{L}$ be the Lagrangian of a field theory and let $|\varphi_0\rangle$ be the ground state of the system. We call a transformation*

$$\begin{aligned} \mathcal{L} &\mapsto \quad \mathcal{L}' \\ |\varphi_0\rangle &\mapsto \quad |\varphi_0'\rangle \end{aligned}$$

an exact symmetry, if both the resulting equations of motion and $|\varphi_0\rangle$ are invariant under this transformation, i.e. $\mathcal{L}' = \mathcal{L} + \alpha\partial_\mu \mathcal{J}^\mu(x)$ for some function $\mathcal{J}^\mu$ and $|\varphi_0\rangle = |\varphi_0'\rangle$.

Definition 2.3.2 (Explicitly broken symmetry) *Let $\mathcal{L}$ be the Lagrangian of a field theory and let $|\varphi_0\rangle$ be the ground state of the system. We call a transformation*

$$\begin{aligned} \mathcal{L} &\mapsto \quad \mathcal{L}' \\ |\varphi_0\rangle &\mapsto \quad |\varphi_0'\rangle \end{aligned}$$

an explicitly broken symmetry, if both the resulting equations of motion and $|\varphi_0\rangle$ are not invariant under this transformation, i.e. $\mathcal{L}' \neq \mathcal{L} + \alpha\partial_\mu \mathcal{J}^\mu(x)$ and $|\varphi_0\rangle \neq |\varphi_0'\rangle$.

Definition 2.3.3 (Spontaneously broken symmetry) *Let $\mathcal{L}$ be the Lagrangian of a field theory and let $|\varphi_0\rangle$ be the ground state of the system. We call a transformation*

$$\begin{aligned} \mathcal{L} &\mapsto \quad \mathcal{L}' \\ |\varphi_0\rangle &\mapsto \quad |\varphi_0'\rangle \end{aligned}$$

a hidden or spontaneously broken symmetry, if the resulting equations of motion are invariant under this transformation but $|\varphi_0\rangle$ is not, i.e. $\mathcal{L}' = \mathcal{L} + \alpha\partial_\mu \mathcal{J}^\mu(x)$ and $|\varphi_0\rangle \neq |\varphi_0'\rangle$.

From this definition follows, that the ground state of a system containing spontaneous symmetry breaking has less symmetries than the Lagrangian itself. A classic example for this is a ferromagnet. The spin-spin interactions of a ferromagnet are invariant under all spacial rotations, which means that the system's Lagrangian as well as its Hamiltonian are $SO(3)$ invariant. If the temperature of the ferromagnet is lower than its Curie temperature $T < T_c$, it has a non vanishing magnetization $\vec{M}$, which obliterates at temperatures higher than the Curie temperature. Since the magnetization has a well defined direction, all rotation other than around the magnetization's axis do not leave the ground state invariant. This means that the ground state only has a $SO(2)$ symmetry left. Another common phenomenon of spontaneously broken symmetries is that the ground state is degenerate. This means that there are multiple realizations for the state of lowest energy, which can be transformed into each other.[3] In the case of the ferromagnet this degeneracy is displayed in a way, that the remaining $SO(2)$ symmetry of the ground state allows the magnet to be rotated around the magnetization's axis without changing the states energy.

2.3.2 Chiral symmetry

Besides spin, color, helicity and other abstract properties a particle can have, an additional property, the *chirality*, is of particular interest in QCD. To investigate this property we first take a look at the fermionic part of the QCD Lagrangian (2.13). If we only consider the lightest u and d quarks, the Lagrangian simplifies to [2]

$$\mathcal{L} = i\overline{u}\not{D}u + i\overline{d}\not{D}d - m_u\overline{u}u - m_d\overline{d}d, \tag{2.17}$$

[3] In most cases these transformations are continuous, although there are also cases, where the realizations of the ground state are connected via discrete transformations.

where u, d and $\overline{u}$, $\overline{d}$ are the fields and the adjoined fields of the u and d quarks. Since the current masses of the u and d quarks are very light compared to the strength of the strong interaction, it seems appropriate to further simplify the Lagrangian by making the approximation $m_u = m_d = 0$. This approximation is called the *chiral limit* and it indeed gives suitable results in most calculations. In the chiral limit the QCD Lagrangian only consists of the terms

$$\mathcal{L} = \overline{u} i \not{D} u + \overline{d} i \not{D} d. \tag{2.18}$$

We can see, that this Lagrangian has isospin symmetry, the symmetry of an $U(2)$ transformation mixing the u and d fields. Additionally, the Lagrangian for massless quarks also contains no coupling between left- and right-handed quarks, so the Lagrangian is actually symmetric under separate transformations for both chiralities

$$\begin{pmatrix} u \\ d \end{pmatrix}_L \to U_L \begin{pmatrix} u \\ d \end{pmatrix}_L, \qquad \begin{pmatrix} u \\ d \end{pmatrix}_R \to U_R \begin{pmatrix} u \\ d \end{pmatrix}_R. \tag{2.19}$$

In above equation U_L and U_R both denote $U(2)$ transformations. Using some group theory we can further separate the $U(2)$ symmetries into a $SU(2) \times U(1)$ symmetry.[4] With that the full symmetry group of the Lagrangian for massless quarks is $SU(2)_L \times SU(2)_R \times U(1)_V \times U(1)_A$. The $SU(2)_L$ and $SU(2)_R$ symmetries are called *chiral symmetries*, the $U(1)_V$ and $U(1)_A$ symmetries are the *vector* and *axial* symmetries. We can take a look at the conserved currents of these symmetries. To do this, we first define a quark doublet with the components

$$Q_L = \left(\frac{\mathbb{1} - \gamma^5}{2} \right) \begin{pmatrix} u \\ d \end{pmatrix}, \qquad Q_R = \left(\frac{\mathbb{1} + \gamma^5}{2} \right) \begin{pmatrix} u \\ d \end{pmatrix}. \tag{2.20}$$

Using these definitions we can further define the currents

$$j_L^\mu = \overline{Q}_L \gamma^\mu Q_L, \qquad j_R^\mu = \overline{Q}_R \gamma^\mu Q_R, \tag{2.21}$$

$$j_L^{\mu a} = \overline{Q}_L \gamma^\mu \tau^a Q_L, \qquad j_R^{\mu a} = \overline{Q}_R \gamma^\mu \tau^a Q_R, \tag{2.22}$$

where $\tau^a = \frac{\sigma^a}{2}$ are the generators of the $SU(2)$ group. If we add up the left- and right-handed currents, we get the conserved baryon number and isospin currents

[4] In general it is possible to separate $U(N)$ symmetries via $U(N) \to SU(N) \times U(1)$, since we can always find a homomorphism that maps $SU(N) \times U(1)$ to $U(N)$, i.e. $f : SU(N) \times U(1) \to U(N) : (S, e^{i\varphi}) \mapsto e^{i\varphi} S$.

$$j^{\mu} = \overline{Q}\gamma^{\mu}Q, \qquad j^{\mu a} = \overline{Q}\gamma^{\mu}\tau^{a}Q, \tag{2.23}$$

which correspond to the chiral symmetry. We can subtract the currents in eq. (2.21) to get the conserved currents of the vector and axial symmetries

$$j^{\mu 5} = \overline{Q}\gamma^{\mu}\gamma^{5}Q, \qquad j^{\mu 5a} = \overline{Q}\gamma^{\mu}\gamma^{5}\tau^{a}Q. \tag{2.24}$$

The symmetries discussed in this section can be generalized from $SU(2) \times U(1)$ symmetries to $SU(3) \times U(1)$ symmetries when including the s quark. Applying the approximation of the chiral limit can still be justified when including the third flavour of quarks as the mass of the s quark is also small compared to the scale of the strong interaction. In fact the ratios of the light quark masses $m_u : m_d : m_s$ are estimated to be $1 : 2 : 40$ [3].

Spontaneous breaking of chiral symmetry

Now that we have discussed spontaneous breaking of symmetries in general, we will have a look at how the chiral symmetry of QCD is broken spontaneously. But before we investigate the consequences of the broken symmetry, we will first ask us why we might expect the chiral symmetries to be broken spontaneously. In QCD quarks and antiquarks have a strong attractive interaction. When these quarks are massless or have a very low mass, the energy required to create a new quark-antiquark pair is small compared to the scale of the interaction between them. Because of this we can expect the QCD vacuum to contain a condensate of quark-antiquark pairs. These pairs have zero net momentum and angular momentum, so they must have a non zero net chiral charge, pairing left-handed quarks and right-handed antiquarks. This condensate is characterized by a finite vacuum expectation value of the operator[5]

$$\left\langle \overline{Q}Q \right\rangle \equiv \left\langle 0 \left| \overline{Q}Q \right| 0 \right\rangle = \left\langle 0 \left| \overline{Q}_L Q_R + \overline{Q}_R Q_L \right| 0 \right\rangle \neq 0. \tag{2.25}$$

We will further denote the value $\left\langle \overline{Q}Q \right\rangle$ simply as *chiral quark condensate*. A non zero chiral quark condensate signals a spontaneously broken chiral symmetry, which allows mixing of the two quark chiralities. This further allows quarks to move through the vacuum whilst acquiring effective masses higher than their current quark masses, even when they have zero mass in the QCD Lagrangian. An important consequence of the chiral limit is Goldstone's theorem, which states

[5] Our considerations follow those of [2].

that for every spontaneously broken, continuous symmetry a massless boson field arises.[6] For QCD these bosons are, as we will see later, the pions. Experiments show that the masses of the pions are in fact non zero, which means that the current quark masses for u and d quarks cannot be zero in reality.

We can express the matrix element of the current $j^{\mu 5a}$ between the vacuum and an on-shell pion as [4]

$$\langle 0| j^{\mu 5a}(x) \left|\pi^b(p)\right\rangle = -ip^\mu f_\pi \delta^{ab} e^{-ipx}, \tag{2.26}$$

with a and b being isospin indices and p^μ is the momentum of the pion. In the above equation, the value f_π is a scalar value of dimension MeV. It is the pions electroweak decay constant, which we will calculate in this thesis in the Bethe-Salpeter formalism. Furthermore, if we contract this equation with p_μ from the left we get

$$\langle 0| p_\mu j^{\mu 5a} \left|\pi^b(p)\right\rangle = -ip^2 f_\pi e^{-ipx} = 0, \tag{2.27}$$

since $j^{\mu 5a}$ is conserved in the chiral limit, i.e. $p_\mu j^{\mu 5a} \equiv \partial_\mu j^{\mu 5a} = 0$. This means, that an on-shell pion must satisfy $p^2 = -m_\pi^2 = 0$, so they are indeed the massless bosons predicted by Goldstone's theorem. If we reintroduce the quark masses into our Lagrangian, $j^{\mu 5a}$ is no longer conserved. As a result the pion mass is actually non zero but satisfies the Gell-Mann-Oakes-Renner relation [4]

$$f_\pi^2 m_\pi^2 = -2m_c \left\langle \overline{Q}Q \right\rangle / N_f \tag{2.28}$$

with N_f being the number of quark flavours. Extending our model to also contain s quarks, additional scalar mesons occur from the breaking of the $SU(3) \times SU(3)$ symmetry, as illustrated in fig. 2.2. In general, the number of occurring Goldstone bosons is equal to the number of degrees of freedom lost due to the spontaneous symmetry breaking.

2.4 The Dyson-Schwinger equations

The Dyson-Schwinger equations (DSE's) are an infinite set of coupled integral equations that describe the propagation of the particles of a quantum field theory. In QCD there are DSE's for the quark, gluon and ghost propagators as well as the quark-gluon, gluon-gluon and ghost-gluon vertices. Since the full set of DSE's

[6] Due to the importance of this theorem, a proof of it is given in section B.1.

$$SU(2) \times SU(2) \xrightarrow{\pi^{0,\pm}} SU(2)$$
$$SU(3) \times SU(3) \xrightarrow[K^{0,\pm}, \overline{K}^0, \eta]{} SU(3)$$

Figure 2.2: The boson occurring due to spontaneously broken chiral symmetry. The bosons in the case $N_f = 3$ occur additionally to the pions.

generally can not be solved in closed form we will have to apply some form of truncation to them. In this thesis we will use a truncation scheme, in which the gluon-propagator and the quark-gluon vertex greatly simplify and do not interact with any ghost propagators, so that we only have to take care of the quark DSE.

Due to the gluon-gluon interactions discussed at the end of section 2.2, a quark can propagate in many ways. The elementary, one-particle irreducible interactions in the Feynman diagrams are conveniently summarized as the *quark self energy* $\Sigma(p)$. In Feynman diagrams, the quark DSE is given in fig. 2.3.

Figure 2.3: The quark DSE expressed in Feynman diagrams. Straight lines correspond to a free quark propagator, lines with an arrow correspond to a dressed quark propagator. Only one vertex is renormalized to avoid double counting.

If we translate the diagram into an explicit formula for the full, "dressed" quark propagator, we get [5]

$$S(p) = S_0(p) + S_0(p)\Sigma(p)S(p), \tag{2.29}$$

where $S_0(p)$ is the free quark propagator and $S(p)$ is the dressed quark propagator. If we write out the sum in full and express it as a geometric series, we get an equation for the inverse quark propagator

$$S^{-1}(p) = S_0^{-1}(p) - \Sigma(p). \tag{2.30}$$

This equation, known as the *gap equation*, can also be expressed in Feynman diagrams, see fig. 2.4. For a derivation of the gap equation, B.2 can be consulted. The free quark propagator is a two point Green's function. If we ignore color, flavour and spin indices, it is given by

$$S_0(p) = \left(m_c + i\not{p}\right)^{-1}, \tag{2.31}$$

where m_c is the current quark mass. We can get the full propagator by dressing the free propagator with dressing functions $A(p^2)$ and $B(p^2)$ via [6]

$$S(p) = \left(B(p^2) + i\not{p}A(p^2)\right)^{-1}. \tag{2.32}$$

If we further introduce the quark mass function $M(p^2) = B(p^2)/A(p^2)$, the dressed propagator can be written as

$$S(p) = A^{-1}(p^2)\frac{-i\not{p} + M(p^2)}{p^2 + M^2(p^2)}. \tag{2.33}$$

Later we will interpret the value of $M(p^2)$ as the effective quark mass. Plugging the expression for the free propagator together with the full quark self energy [7] back into the eq. (2.30) yields the explicit form of the gap equation

$$S^{-1}(p) = i\not{p} + m_c + g^2\frac{4}{3}\int \frac{\mathrm{d}^4q}{(2\pi)^4}\gamma_\mu S(q)\Gamma_\nu(q,p)D^{\mu\nu}(p-q), \tag{2.34}$$

where g is the coupling strength already introduced in section 2.2, $D^{\mu\nu}(p-q)$ denotes the dressed gluon propagator and $\Gamma_\nu(q,p)$ is the full quark-gluon vertex. The factor $4/3$ stems from the trace of the color Gell-Mann matrices. The expression for the quark self energy can be obtained using the Feynman rules of QCD, i.e. the emission of the gluon at the point μ at a bare vertex corresponds to a γ_μ, the fermion line corresponds to the full quark propagator $S(q)$, the absorption at the dressed vertex at point ν corresponds to the full quark-gluon vertex Γ_ν and finally the boson line gives the gluon propagator $D^{\mu\nu}$. Since the momentum of the gluon is not fixed by external conditions, it can take any possible value, which is realized by the integration.

Figure 2.4: The gap equation expressed in Feynman diagrams. Compared with the DSE the graphs here are one-particle irreducible and consist of no external propagators.

2.5 The Bethe-Salpeter equation

To determine the properties of bound states of quarks and antiquarks, in our case mesons, we need to consult a more complicated formalism, since we also need to consider all possible interactions between the quarks. This formalism obviously has to contain the solutions of the quark DSE, but it also has to satisfy the *Ward-Takahashi* identities, which will be discussed in section 2.6. The formalism used in this thesis is the Bethe-Salpeter formalism. The idea behind this formalism is, to start with the exact equation for scattering processes in QCD. The interaction is determined by a 4-point Green's function, the full propagator G, which can be expressed by a bare propagator and the scattering T-Matrix, describing the interactions between the quarks, as [8]

$$G = G_0 + G_0 T G_0. \tag{2.35}$$

The scattering T-Matrix satisfies a Dyson equation itself

$$T = K + K G_0 T, \tag{2.36}$$

where K is the scattering kernel. We can choose the ansatz

$$T \propto \frac{\Gamma\overline{\Gamma}}{P^2 + m^2}, \tag{2.37}$$

in which we introduced the *Bethe-Salpeter amplitude* (BSA) Γ and its conjugated amplitude $\overline{\Gamma}$. Using the fact, that in this ansatz T diverges for on-shell particles with the energy-mass-relation $P^2 = -m^2$, eq. (2.36) simplifies to

$$\Gamma = K G_0 \Gamma. \tag{2.38}$$

For a full derivation, section B.3 can be consulted. This equation is called the *Bethe-Salpeter* equation. It is an eigenvalue equation of the matrix KG_0 with the eigenvalue 1. Thus, every state Γ_0 which satisfies eq. (2.38) has the potential to represent a physical state of the meson. The BSE can be written as an explicit integral equation [9]

$$\left[\Gamma^j(p,P)\right]_{tu} = \int \frac{\mathrm{d}^4 q}{(2\pi)^4} K^{rs}_{tu}(q,p,P) S(q_+) [\Gamma^j(q,P)]_{sr} S(q_-). \tag{2.39}$$

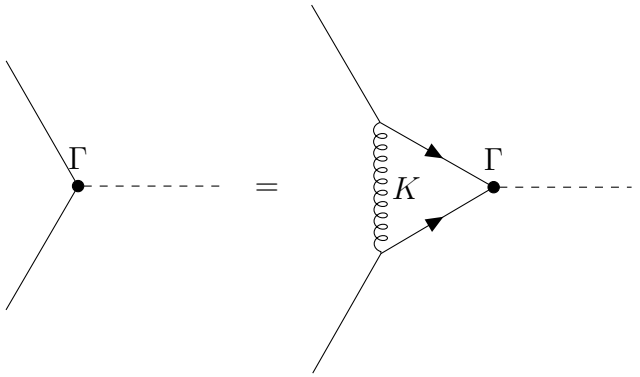

Figure 2.5: The Bethe-Salpeter equation in Feynman diagrams. The two quark propagators denote the quark and antiquark respectively, the kernel K contains each possible interaction between the quarks.

In this equation, p is the relative and P is the absolute momentum of the meson. The indices j, r, s, t and u are color, flavour and Dirac indices. The momenta of the quarks are given by $q_+ = q + \eta P$ and $q_- = q + (\eta - 1)P$. The routing parameter η ranges from 0 to 1 and determines, how much of the meson's momentum is carried by each constituents. As it only varies internal momenta of the meson, observable quantities should be independent of η. The general solution of the BSE is given by [10]

$$\Gamma^\mu(p,P) = -\frac{4g^2}{3}\int \frac{\mathrm{d}^4 q}{(2\pi)^4} D^{\mu\nu}(p-q)\gamma_\mu S(q_+)\Gamma^\mu(q,P)S(q_-)\Gamma^{\mathrm{qg}}_\nu(q,p). \quad (2.40)$$

We gave the quark-gluon vertex the additional label "qg" to distinguish it from the BSA. This integral equation can again be derived from the diagrammatic equation displayed in fig. 2.5 using the Feynman rules of QCD. As in the gap equation, only one quark-gluon vertex has to be dressed, while the other one corresponds to the bare vertex factor γ_μ.

To solve the Bethe-Salpeter equation, we choose the ansatz to express the amplitude as a linear combination of the underlying Dirac structures, which can be taken from [11]

$$\Gamma(p,P) = \gamma_5[\mathbb{1}\cdot E(p,P) - i\not{P}F(p,P) - i\not{p}G(p,P) - i[\not{P},\not{p}]_- H(p,P)]. \quad (2.41)$$

After applying a truncation scheme, we will be able to solve the BSE algebraically using this ansatz.

As an abstract, mathematical quantity from which physical quantities should be determined, the BSA has to have a well defined normalization condition, since

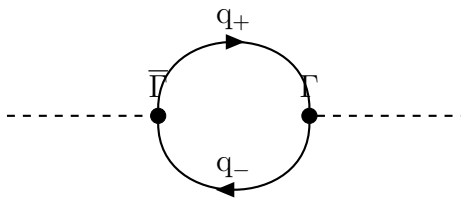

Figure 2.6: The normalization condition (2.42) expressed as a Feynman diagram.

multiplying it by a arbitrary complex number keeps the BSE invariant.[7] The normalization condition reads

$$\overline{\Gamma}\left[\frac{\mathrm{d}G_0}{\mathrm{d}P^2} + G_0\frac{\mathrm{d}K}{\mathrm{d}P^2}G_0\right]\Gamma = -1, \tag{2.42}$$

which is obtained by taking the derivative of G. If the scattering kernel K is independent of P, the second term vanishes. If we further split G_0 into two 2-point Green's functions, the normalization condition simplifies to

$$\overline{\Gamma}\left[\frac{\mathrm{d}G_{(2)}G_{(2)}}{\mathrm{d}P^2}\right]\Gamma = -1. \tag{2.43}$$

This condition can also be expressed in Feynman diagrams, as seen in fig. 2.6. We can, again using the Feynman rules of QCD, translate this into an explicit integral equation

$$1 = \frac{\mathrm{d}}{\mathrm{d}P^2}\,\mathrm{tr}\int\frac{\mathrm{d}^4q}{(2\pi)^4}\overline{\Gamma}(q,K)S(q_+)\Gamma(q,K)S(q_-). \tag{2.44}$$

Note, that the inner momentum q needs to be integrated over and due to the implicitness of the equation, the trace over all color, flavour and Dirac indices needs to be taken. With the properly normalized BSA we are able to calculate the pion's leptonic decay constant. To do this, we express eq. (2.26) in momentum space, which yields [12]

$$\delta^{ij}f_\pi P_\mu = Z_2\int\frac{\mathrm{d}^4q}{(2\pi)^4}\,\mathrm{tr}\left[\frac{\sigma^i}{2}\gamma_5\gamma_\mu S(q_+)\Gamma^j(q,P)S(q_-)\right], \tag{2.45}$$

with Z_2 being a renormalization constant.

[7] This is analogous to classical quantum mechanics, where the solutions of the Schrödinger equation $H\left|\psi\right\rangle = i\partial_t\left|\psi\right\rangle$ have to be normalized by the condition $\langle\psi|\psi\rangle = 1$.

2.6 Truncation schemes

In general, solving the full set of Dyson-Schwinger equations of QCD is not possible in closed form. Because of this, truncation schemes have to be applied to approach challenging problems like the dynamic mass generation of quarks and mesons. One possible truncation is to apply simplifications to the quark-gluon vertex. This simplifies the relevant equations to ones containing only terms that can be handled more easily. However, these truncation schemes can not be chosen arbitrary, but have to satisfy certain identities, the *Ward-Takahashi* identities. In our case, the axial vector Ward-Takahashi identity (AVWTI) is of particular interest, as it ensures, that the effects of the spontaneously broken chiral symmetry are preserved. It provides a connection between the interactions used in the quark DSE and the meson BSE. In its explicit form the AVWTI is given by

$$\gamma^5\Sigma(q_-) + \Sigma(q_+)\gamma^5 = -\int K(p,q,P)(\gamma^5 S(q_-) + S(q_+)\gamma^5). \tag{2.46}$$

We see, that the AVWTI indeed gives a relation between the quark self energy Σ and the scattering kernel K, which is part of the meson BSE. If we violate this relation in our choice of truncation schemes, problems will arise.

2.6.1 The Rainbow-Ladder truncation

The truncation scheme used in this thesis is an often used one, called the *Rainbow-Ladder* truncation. The idea behind it is to replace the full quark-gluon vertex by a simplified one. This allows the quark to simply emit one gluon and absorb it equivalently. This means, that both the vertex, at which the gluon is emitted, and the one, at which it is absorbed again, are both described as a bare vertex. While one gluon is emitted and propagating, more gluons may be emitted and absorbed. Additionally, we use a simplified contact interaction model, which not only ensures that the emitted gluons propagate freely, not interacting with each other, but also further simplifies the gluon propagator. The name stems from the fact that after applying the truncation scheme, the remaining Feynman diagrams in the quark DSE look like rainbows, which are getting bigger for higher order terms, see fig. 2.7.

Effects on the quark DSE

As mentioned in section 2.4, the gluon propagator and the quark-gluon vertex also obey their own set of Dyson-Schwinger equations and are accordingly complicated as well. This is where the Rainbow-Ladder truncation leads to simplifications. In

general, the quark-gluon vertex can be expressed with the aid of three independent four vectors and the four Dirac structures [7] introduced in section 2.5, such that

$$\Gamma^\mu \in \{\gamma^\mu, p^\mu, q^\mu\} \otimes \{\mathbb{1}, p\!\!\!/, q\!\!\!/, [p\!\!\!/, q\!\!\!/]_-\}. \tag{2.47}$$

In Rainbow-Ladder truncation, we only consider the first term $\gamma^\mu \otimes \mathbb{1}$, such that the quark-gluon vertex is given by a bare vertex factor, i.e.

$$\Gamma^\mu(q, p) = \gamma^\mu. \tag{2.48}$$

The full gluon propagator in Landau gauge is then given by [8]

$$D^{\mu\nu}(k) = \left(\delta^{\mu\nu} - \frac{k^\mu k^\nu}{k^2}\right) \frac{Z(k^2)}{k^2}. \tag{2.49}$$

We simplify the interaction further by first assuming the function $Z(k^2)$ to be constant. Furthermore we choose a contact interaction of the form [10]

$$D^{\mu\nu} = \frac{\delta^{\mu\nu}}{g^2 m_G^2}, \tag{2.50}$$

where m_G is the *gluon mass scale*, which quantifies the interaction strength. Since the gluon propagator is dependent on the value of m_G, we expect the effective quark mass to also depend on it. If we plug the truncated quark-gluon vertex and gluon-propagator into the gap equation (2.34), it simplifies to

$$S^{-1}(p) = i p\!\!\!/ + m_c + \frac{4}{3m_G^2} \int \frac{\mathrm{d}^4 q}{(2\pi)^4} \gamma_\mu S(q) \gamma^\mu, \tag{2.51}$$

which can be solved iteratively after further simplifications using the relations of the gamma matrices mentioned in section A.2.

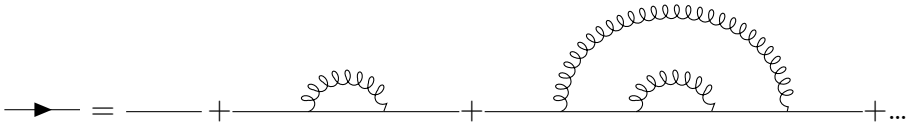

Figure 2.7: The quark propagator in Rainbow-Ladder truncation. The high order diagrams closely resemble rainbows, which inspired the name of the truncation scheme.

Effects on the Bethe-Salpeter equation

The part of the Bethe-Salpeter equation, that will be affected by the truncation, is the scattering kernel K, which describes how gluons are exchanged between the constituents of the meson. In order not to violate the AVWTI, the gluon propagator and quark-gluon vertex used in the quark DSE have to be used here, too. This leads to a significant simplification of the possible interactions to the exchange of only one freely propagating gluon at once between the quarks. Iterating the BSE with these approximations leads to Feynman diagrams that look like a ladder with steps made of gluons (fig. 2.8).

Plugging the truncated quark-gluon vertex $\Gamma^\mu = \gamma^\mu$ and the gluon propagator with the contact interaction $D^{\mu\nu} = \delta^{\mu\nu}/g^2 m_G^2$ into the integral form of the BSE (2.40) yields

$$\Gamma^\mu(P) = -\frac{4}{3m_G^2}\int \frac{\mathrm{d}^4 q}{(2\pi)^4}\gamma^\nu S(q_+)\Gamma^\mu(P)S(q_-)\gamma_\nu. \tag{2.52}$$

Since we used a simple form for the gluon propagator, that does not depend on the relative momentum p, the Bethe-Salpeter amplitude itself does no longer depend on p. Thus, our ansatz (2.41) simplifies, as the last two terms vanish. So the Bethe-Salpeter amplitude only has two degrees of freedom, E and F, that need to be determined, and is given by [10]

$$\Gamma(P) = \gamma^5\left[iE(P) + \frac{\not{P}}{M}F(P)\right]. \tag{2.53}$$

The two additionally inserted factors i and $1/M$ are convention dependent, so that the values for the BSA might differ source-by-source, but as long as observable

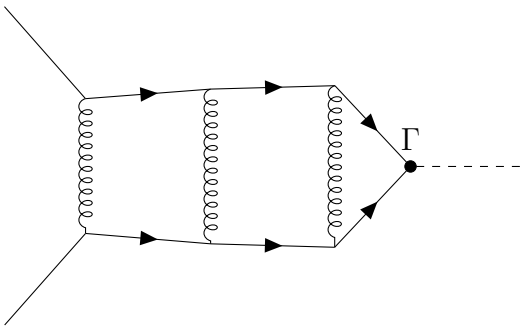

Figure 2.8: The Bethe-Salpeter amplitude in Rainbow-Ladder truncation after three iterations of eq. (2.38).

quantites, such as the mass m_π of the pion, are the same, this does not matter. Plugging eq. (2.53) into eq. (2.52), leads to the eigenvalue equation

$$\begin{pmatrix} \kappa_{EE} & \kappa_{EF} \\ \kappa_{FE} & \kappa_{FF} \end{pmatrix} \begin{pmatrix} E \\ F \end{pmatrix} = \lambda(m_\pi) \begin{pmatrix} E \\ F \end{pmatrix}, \tag{2.54}$$

which can be solved algebraically. For a derivation of this equation, section B.3 can be consulted. To determine the correct mass of the pion, we have to vary it until the eigenvalue $\lambda(m_\pi)$ is equal to 1. The 2×2 matrix in above equation still depends on the four-momentum $P^\mu = \left(i\sqrt{m_\pi^2 + \vec{p}^{\,2}}, \vec{p}\right)$, so that in principle the mass of the pion might still depend on the three-momentum $\vec{p}$. Weather this is indeed the case will be investigated later, when we solve the BSE in a moving frame.

Chapter 3

Pion in its restframe

3.1 Solving the gap equation

3.1.1 Mathematical approach

As we have already seen in section 2.6, the gap equation becomes significantly simpler in Rainbow-Ladder truncation using the contact interaction (2.50)

$$S^{-1}(p) = i\not{p} + m_c + \frac{4}{3m_G^2}\int \frac{\mathrm{d}^4q}{(2\pi)^4}\gamma_\mu S(q)\gamma^\mu. \tag{3.1}$$

To solve this equation, we plug our ansatz (2.32) into it to obtain

$$i\not{p}A(p^2) + B(p^2) = i\not{p} + m_c + \frac{4}{3m_G^2}\int \frac{\mathrm{d}^4q}{(2\pi)^4}\gamma_\mu \frac{-i\not{q}A(q^2) + B(q^2)}{q^2A^2(q^2) + B^2(q^2)}\gamma^\mu. \tag{3.2}$$

Using the relations of the gamma matrices, we can solve this equation for $A(p^2)$ and $B(p^2)$. A full derivation is given in section B.2. Here we will only recall the resulting equation for the effective quark mass $M(p^2) = B(p^2)/A(p^2)$. For A we obtained the result $A(p^2) = 1$. As a consequence the effective quark mass becomes independent of the momentum p and is given by

$$M = m_c + \frac{1}{3m_G^2\pi^2}\int_0^\infty \mathrm{d}s \frac{sM}{s + M^2}. \tag{3.3}$$

If we take a closer look at the asymptotic behaviour of the function inside the integral, we see, that it does not converge to zero as x goes to infinity, but rather

$$\lim_{x\to\infty} \frac{xM}{x+M^2} = M \neq 0. \tag{3.4}$$

A necessary condition for an improper integral to converge is, that the function, which is integrated, has to go to zero almost everywhere as x goes to infinity. Since this is not the case for our function, the integral in equation (3.3) diverges. This is a typical phenomenon in quantum field theories, that has to be worked around. The procedure of modifying divergent integrals to get meaningful results is called *regularization.* The simplest way to modify the divergent integral is to introduce a hard cutoff parameter Λ, such that we replace the improper integral with

$$\int_0^\infty \mathrm{d}s \frac{sM}{s+M^2} \qquad \longrightarrow \qquad \int_0^\Lambda \mathrm{d}s \frac{sM}{s+M^2}. \tag{3.5}$$

Since the function we are integrating over is bound in any compact interval $q \in [0, \Lambda]$, this expression is well defined. This method has the advantage of being easy to implement and giving good results for the effective quark mass. The problem of this method is, that it violates the integrals invariance under translations. This will cause some issues when solving the pion BSE later. Therefore, we have to find a different approach to regularization. The next idea would be to modify the integrated function itself in such a way, that it goes to zero fast enough to ensure convergence of the integral. To do this, we use the identity

$$\frac{1}{s+M^2} = \int_0^\infty \mathrm{d}\tau e^{-(s+M^2)\tau}. \tag{3.6}$$

Now we can modify this integral by replacing the limits of integration with finite values to properly regularize the problem [13]

$$\int_0^\infty \mathrm{d}\tau e^{-(s+M^2)\tau} \to \int_{\tau_{uv}^2}^{\tau_{ir}^2} \mathrm{d}\tau e^{-(s+M^2)\tau} = \frac{e^{-(s+M^2)\tau_{uv}^2} - e^{-(s+M^2)\tau_{ir}^2}}{s+M^2}, \tag{3.7}$$

where τ_{uv} and τ_{ir} are ultraviolet and infrared regulators respectively. With these regulators, the function decays exponentially for big values of s so it becomes integrable in $\mathbb{R}^+$. In this thesis we will calculate the effective quark mass with

both regularizations once. We solve equation (3.3) iteratively using numerical integration, the Gauß-Legendre method in particular.[1] In a first calculation, its dependence on the current quark mass m_c will be analyzed, in a second calculation we will investigate the effects of a varying gluon mass scale m_G on the effective quark mass at a fixed value of m_c.

The results of these calculations can be used to calculate the chiral quark condensate $\langle \overline{Q}Q \rangle$, which has already been introduced in section 2.3.2. The value of $\langle \overline{Q}Q \rangle$ can be determined by [8]

$$\langle \overline{Q}Q \rangle = \mathcal{N} N_c \int \frac{\mathrm{d}^4 q}{(2\pi)^4} \operatorname{tr}(S_{chiral}(q)), \tag{3.8}$$

where $S_{chiral}(q)$ is the quark propagator in the chiral limit $m_c = 0$ and $\mathcal{N} = Z_2 Z_m$ is a renormalization constant. An explicit calculation yields a relation[2] between $\langle \overline{Q}Q \rangle$, M and m_c

$$\langle \overline{Q}Q \rangle / \mathcal{N} = \frac{9}{4} m_G^2 (M - m_c). \tag{3.9}$$

Using this relation we will be able to calculate the chiral quark condensate and if its value is non vanishing, we know that chiral symmetry is broken spontaneously.

3.1.2 Numerical results

To get the relation $M(m_c)$, equation (3.3) has been iterated for 1000 equidistant values of m_c in the interval $[0, 10]$ until an accuracy of 10^{-7} is reached.[3] A gluon mass scale of $m_G = 132.0\,\mathrm{MeV}$ was used, together with a hard ultraviolet cutoff parameter of $\Lambda = 873\,\mathrm{MeV}$. The results are plotted in figure 3.1a.

One sees, that for light quarks the effective masses are way bigger than their current masses. The ratio between the effective and current quark masses is also plotted in figure 3.1b. Especially for very light quarks, such as the u and d quarks[4], the effective masses outweigh the current masses by a factor of over 100. This correlates well with the example given in the introduction, the proton, where about 99% of the mass is generated dynamically. We have to keep in mind though, that we only included light quarks in our calculations and left the heavier quarks, such as the c, b and t quarks with masses up to over $150\,\mathrm{GeV}$ for the t quark [1].

[1] All numerical methods and tools used in this thesis are explained in section C of the appendix.
[2] For a derivation of this relation, B.4 can be consulted.
[3] If not explicitly stated otherwise, all masses, momenta and energies are given in MeV.
[4] $m_u \approx 2.3\,\mathrm{MeV}$, $m_d \approx 4.8\,\mathrm{MeV}$

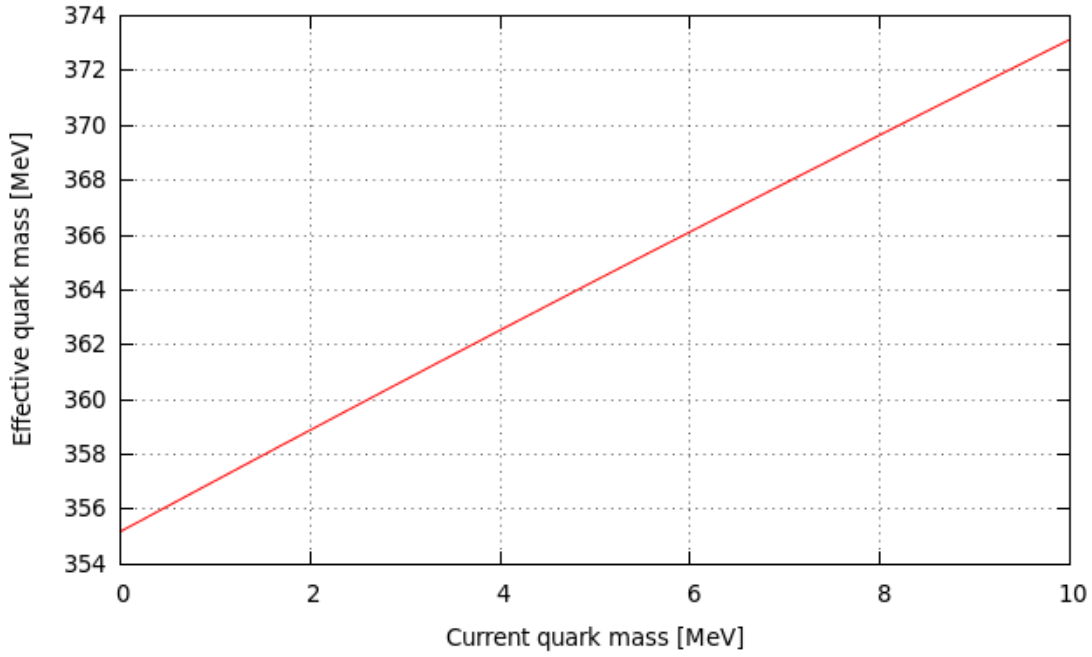

(a) The relation $M(m_c)$ with $m_c \in [0, 10]$MeV.

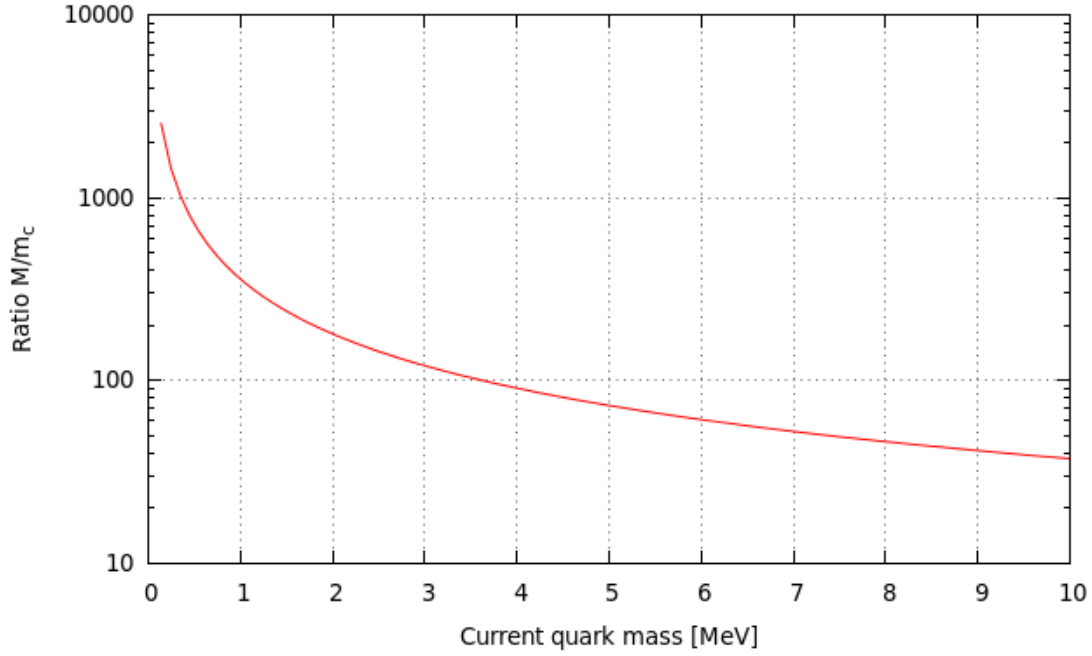

(b) The ratio M/m_c plotted on a logarithmic scale.

Figure 3.1

An astonishing result is that even in the chiral limit the quarks can dynamically generate an effective mass of about 355.18 MeV, even though their current mass is zero. This raises the question how the mass is generated in the first place. Searching for an answer one may vary the interaction strength and research the behaviour of $M(m_G)$. To be more precise, the value for m_G^{-2}, as it appears in eq. (3.3), is varied in an interval of $[0, 70]\,\mathrm{GeV}^{-2}$. In the previous calculation its value was fixed to a value that reproduces the experimental values for the pions properties, as we will see when discussing the results of the BSE. In figure 3.2a, the results of this calculation are plotted once for the chiral limit and once for a fixed value of $m_c = 7.8\,\mathrm{MeV}$.

The behaviour of the effective quark mass is very interesting. In the chiral limit, the effective mass is zero for small values of m_G^{-2}, i.e. for large m_G. This observation holds true up to a critical value of the gluon mass scale of $m_G^{-2} \simeq 38.9\,\mathrm{GeV}^{-2}$, which corresponds to a critical value for $m_G^{\mathrm{crit}} \simeq 160.3\,\mathrm{MeV}$. For bigger m_G^{-2}, the effective quark mass harshly increases, even though the current mass is still zero. If we consider a non vanishing current mass of $m_c = 7.8\,\mathrm{MeV}$, the effective quark mass approaches the current mass in the limit $m_G \to \infty$. In contrast to the chiral limit though, the effective mass slightly increases for increasing value of m_G^{-2}, that are still smaller than the critical value of $39\,\mathrm{GeV}^{-2}$. At the critical point the effective

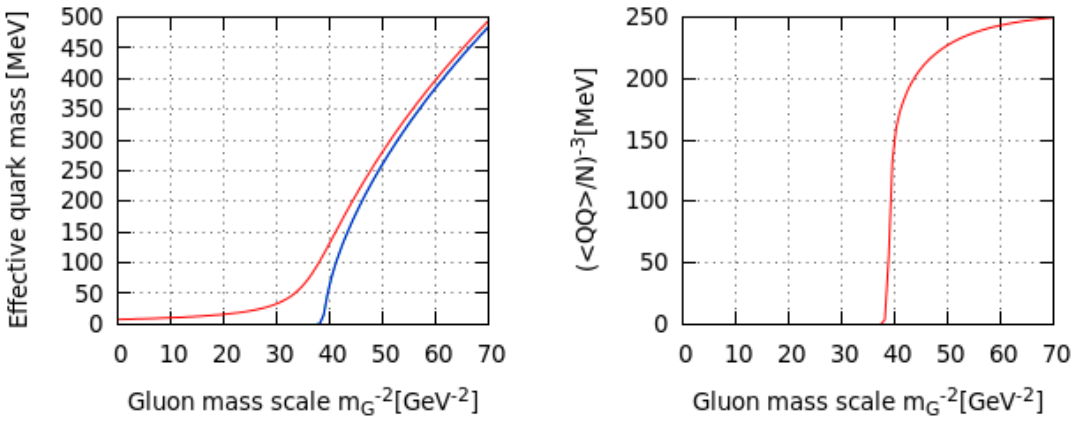

(a) The effective quark mass plotted against the gluon mass scale. The upper plot is for $m_c = 7.8\,\mathrm{MeV}$, the lower is for the chiral limit.

(b) The chiral quark condensate plotted against the gluon mass scale. For simplicity's sake, the renormalization constant $\mathcal{N}$ has been omitted.

Figure 3.2: Behaviour of the effective quark mass (left panel) and the chiral quark condensate (right panel) under variation of the interaction strength. One can see, that the values for both harshly start to increase at $m_G^{-2} \approx 38.9\,\mathrm{GeV}^{-2}$.

mass also starts to increase faster, indicating that the majority of their mass is then also generated dynamically. This means, that for finite current quark masses, mass is already generated dynamically for small interaction strengths, while in the chiral limit the behaviour of the effective mass can be described as

$$\begin{cases} M = 0, & \text{for } m_G \geq m_G^{\text{crit}} \\ M > 0, & \text{for } m_G < m_G^{\text{crit}}. \end{cases} \tag{3.10}$$

This strange property raises the idea that something special happens at the critical interaction strength m_G^{crit}. In search of this "special thing", the value of the chiral quark condensate $\langle \overline{Q}Q \rangle$ has been calculated for varying interaction strengths. The results are shown in the right plot in fig. 3.2b. The chiral quark condensate indeed shows the same behaviour as the effective quark mass in the chiral limit. If we recall, how the chiral quark condensate was introduced in section 2.3.2, it becomes clear that the non vanishing value of $\langle \overline{Q}Q \rangle$ for $m_G < m_G^{\text{crit}}$ is an indicator, that the chiral symmetry of QCD is broken spontaneously. This leads to the appearance of a condensate in the QCD vacuum, which causes to quarks to generate mass dynamically. If we try to find an analogy to statistical physics,[5] it would be that this spontaneous symmetry breaking represents a second order phase transition between the two phases *chiral symmetric* and *not chiral symmetric*. As stated earlier, we first set $m_G = 132\,\text{MeV}$, so that the experimental value for the pions mass and decay constant can be reproduced later. In other words, the value of $m_G = 132\,\text{MeV}$ can be interpreted as an initial condition of the universe, which sets the hadronic masses to what they actually are, according to experiments. One can easily think of a hypothetical, alternative universe, in which the value for m_G is higher than m_G^{crit}. In this universe dynamic mass generation would not play as much of a role, so that the masses of hadrons are merely the sum of their constituents' masses. This might seem like a meaningless thought, but it is indeed not entirely clear, if fundamental physical constants actually have been constant for the past 13.8 billion years [14].

The fact, that the experimental value of m_G is smaller than the critical value m_G^{crit} supports the notion, that chiral symmetry is broken spontaneously in QCD. Because of this, we expect massless Goldstone bosons to appear, in particular the pions as they are the simplest fundamental bound states of u and d quarks allowed by (2.12). The fact, that the light quarks actually do have a mass can be brought in as a perturbation, as they still are small compared to their effective masses. Thus the effect on the pions mass should be small too.

[5] Many phenomena of quantum field theories have analogous phenomena in statistical physics, as pointed out in [2].

3.2 Solving the Bethe-Salpeter equation

3.2.1 Mathematical approach

When the Bethe-Salpeter equation was introduced in section 2.5 we have seen, that it is an eigenvalue equation to the eigenvalue 1. After applying the Rainbow-Ladder truncation scheme onto the BSE, it simplifies to an eigenvalue equation of a 2×2 matrix

$$\begin{pmatrix} \kappa_{EE} & \kappa_{EF} \\ \kappa_{FE} & \kappa_{FF} \end{pmatrix} \begin{pmatrix} E \\ F \end{pmatrix} = \begin{pmatrix} E \\ F \end{pmatrix}. \tag{3.11}$$

The matrix elements of the κ-matrix have been derived explicitly in section B.3. We will just recall the results here

$$\kappa_{EE} = 4\mathcal{N} \int^{\infty} \mathrm{d}(q,z,y) \frac{(q_+ \cdot q_-) + M^2}{(q_-^2 + M^2)(q_+^2 + M^2)} \tag{3.12}$$

$$\kappa_{EF} = -4m_\pi^2 \mathcal{N} \int^{\infty} \mathrm{d}(q,z,y) \frac{1}{(q_-^2 + M^2)(q_+^2 + M^2)} \tag{3.13}$$

$$\kappa_{FE} = 2M^2 \mathcal{N} \int^{\infty} \mathrm{d}(q,z,y) \frac{1}{(q_-^2 + M^2)(q_+^2 + M^2)} \tag{3.14}$$

$$\kappa_{FF} = -2\mathcal{N} \int^{\infty} \mathrm{d}(q,z,y) \frac{M^2 - m_\pi^{-2}(m_\pi^2 (q_+ \cdot q_-) + 2(q_+ \cdot P)(q_- \cdot P))}{(q_-^2 + M^2)(q_+^2 + M^2)}. \tag{3.15}$$

Analogous to the integral in equation (3.3), the integral in all of the matrix elements have an ultraviolet divergence. Therefore they have to be regularized, too. The first idea would be to reuse the hard ultraviolet cutoff parameter used for the calculation of the effective quark masses. This would replace the upper limit of integration by the parameter Λ, i.e.

$$\int^{\infty} \mathrm{d}(q,z,y) \quad \longrightarrow \quad \int^{\Lambda} \mathrm{d}(q,z,y). \tag{3.16}$$

To some extend this choice might seem reasonable, but we will see, that it actually produces nonphysical results. Therefore, the alternative way of regularizing the integral by giving the integrated function an exponential decay is more adequate. As the pion consists of two quarks with their propagators both contributing to the Bethe-Salpeter amplitude, it is possible to replace either of them by the regularized propagator

$$\frac{1}{(q_-^2+M^2)(q_+^2+M^2)} \longrightarrow \frac{e^{-(q_\pm^2+M^2)\tau_{uv}^2} - e^{-(q_\pm^2+M^2)\tau_{ir}^2}}{(q_-^2+M^2)(q_+^2+M^2)}. \tag{3.17}$$

We will investigate the effects of the different approaches to regularization as well as the effect on regularizing each quark individually in section 3.2.2.

Figure 3.3 shows a Feynman diagram of the Bethe-Salpeter equation with the important momenta explicitly depicted. The momenta q_+ and q_- have been introduced in section 2.5 and satisfy the relation $q_+ - q_- = P$. As we are now only concerned with calculating the pions properties in its rest frame, the total momentum is $P = (im_\pi, 0, 0, 0)$ and satisfies the energy-mass relation of on-shell particles $P^2 = -m_\pi^2$. This makes one of the angular integrals trivial, giving an additional factor of 2. The routing parameter η only quantifies, how much of the pions momentum is carried by each quark individually and does not directly vary the total momentum. Thus we expect the physics not to change when modifying η.

Before solving the BSE for the amplitude (E, F), we have to determine the pions mass. To do this we calculate the eigenvalue of the κ-matrix for different values of m_π. Once the eigenvalue is equal to 1, m_π is equal to the physical pion mass. The correct value of m_π is found using the false position method, see sec. C, to find the zeros of $f(m_\pi) = \lambda(m_\pi) - 1$ with λ being the eigenvalue. Since only one of the eigenvalues of the κ-matrix is relevant, the eigenspace in which the Bethe-Salpeter amplitude exists, is only a one dimensional subspace $\Omega \subset \mathbb{R}^2$. Normalizing the amplitude properly using the normalization condition (2.42) makes the eigenspace collapse down to a well defined tuple $(E, F) \in \mathbb{R}^2$. Bringing the normalization condition into an easier to compute form, we obtain the equation

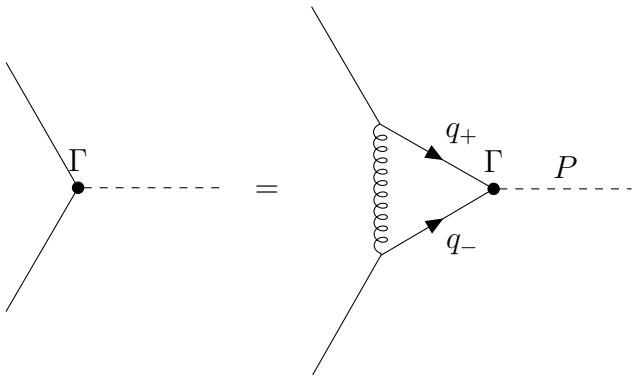

Figure 3.3: The Bethe-Salpeter equation with the relevant momenta.

$$
\begin{aligned}
1 =& \frac{1}{3P\pi^3}\frac{\mathrm{d}}{\mathrm{d}P}\int^{\Lambda}\mathrm{d}(q,z)\Big\{[-M^2-(q_+\cdot q_-)]E^2-2(p\cdot K)EF \\
&+\left[K^2+M^{-2}(2(q_+\cdot K)(q_-\cdot K)-K^2(q_+\cdot q_-))\right]F^2\Big\} \\
&\cdot\left[(q_-^2+M^2)(q_+^2+M^2)\right]^{-1}.
\end{aligned}
$$

A derivation of this equation can be found in section B.5. To clarify the notation, K is equal to the total momentum P, but is denoted with a different letter to highlight that the derivative $\mathrm{d}/\mathrm{d}P$ is not taken with respect to K. Before solving this equation, we first use the eigenvalue condition (3.11) to find the ratio between E and F

$$
\alpha := \frac{F}{E} = \frac{1-\kappa_{EE}}{\kappa_{EF}} \tag{3.18}
$$

and then rewrite the components of the amplitude as $E = 1/N$ and $F = \alpha/N$ with a normalization constant N. Using these notations, the normalization condition is only an equation to determine N. The differentiation with respect to P can either be done analytically or numerically using the method explained in section C. With a properly normalized amplitude, the pions leptonic decay constant can be calculated. Therefore, we bring eq. (2.45) into an easier to handle form[6] and get

$$
f_\pi = \frac{3}{\pi^3}\int^{\Lambda}\mathrm{d}(q,z)\frac{ME-(M^{-1}P^{-2}(2(q_+\cdot P)(q_-\cdot P)-P^2(q_+\cdot q_-)))F}{(q_-^2+M^2)(q_+^2+M^2)}. \tag{3.19}
$$

With the resulting values for m_π and f_π we are furthermore able to test, if the Gell-Mann-Oakes-Renner relation (2.28) holds true in the Rainbow-Ladder truncation with the contact interaction model or if the huge simplifications cause a violation.

3.2.2 Numerical results

Before solving the Bethe-Salpeter equation for the Bethe-Salpeter amplitude, we calculate the correct pion mass to ensure the eigenvalue in the BSE is equal to one. The results for the pion mass for current quark masses varying in the range $m_c \in [0, 10]$ is shown in figure 3.4. The calculations have been done for two different

[6]The derivation is completely analogous to the one done in section B.3.

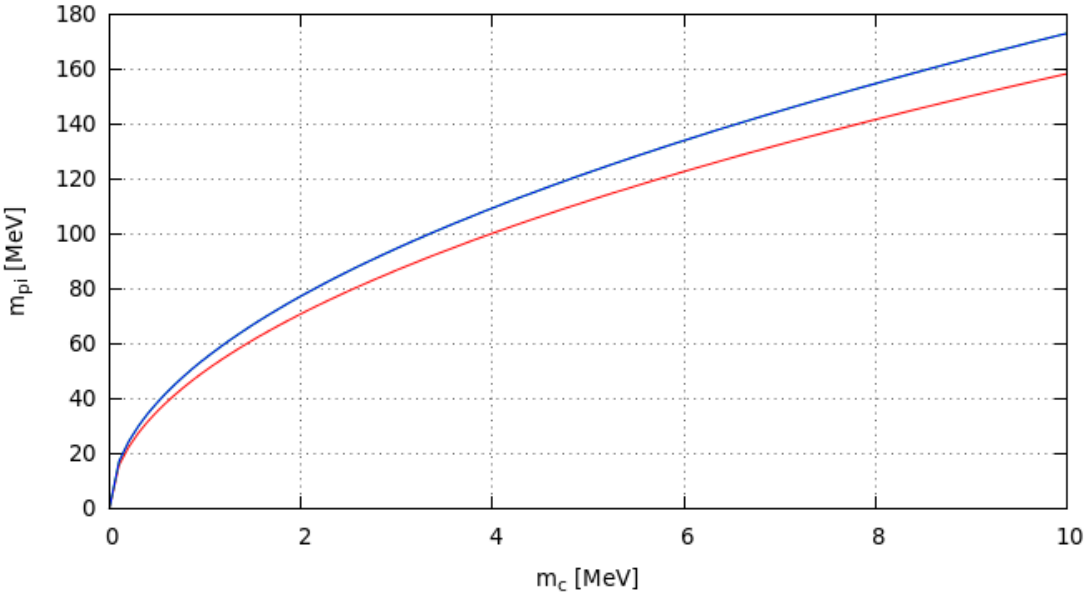

Figure 3.4: The pion mass as a function of the current quark mass.
Upper graph: Symmetric momentum routing $\eta = 0.5$.
Lower graph: Antisymmetric momentum routing $\eta = 1.0$.

momentum routings using the hard cutoff parameter to regularize the integrals. The first one is the symmetric case $\eta = 0.5$, in which the momentum of the pion is equally split between the constituents. The second one is the asymmetric case $\eta = 1.0$, in which one quark carries the full momentum. Even though the routing should not influence the physics of our system, the pion mass is higher in the symmetric case with the difference increasing for higher current quark masses. In fact, the behaviour of the pion mass under variation of the routing parameter closely resembles a parabola. This can be seen in figure 3.5a. This occurs due to the invariance under translations of the integral being violated by the hard cutoff parameter.

To solve this problem, we apply the alternative way of regularizing the integrals occurring in the BSE, which has been introduced in section 3.1.1. To find proper values for the infrared and ultraviolet regulators τ_{ir} and τ_{uv}, we first use this method of regularization to calculate the effective quark mass. It turns out, that the quark masses for both methods match for the values $\tau_{uv} = 1.10562 \cdot 10^{-3}\,\text{MeV}^{-1}$ and $\tau_{ir} = 10^{-5}\,\text{MeV}^{-1}$. For convenience, the inverse values of the regulators $\Lambda_{ir,uv}$ are often used. In our case they are $\Lambda_{ir} = 10^5\,\text{MeV}$ and $\Lambda_{uv} = 904.466\,\text{MeV}$. While the quark mass is sensitive for variations in Λ_{uv}, variations in Λ_{ir} do not change the result as much, as long as it is reasonably large. The same calculations to

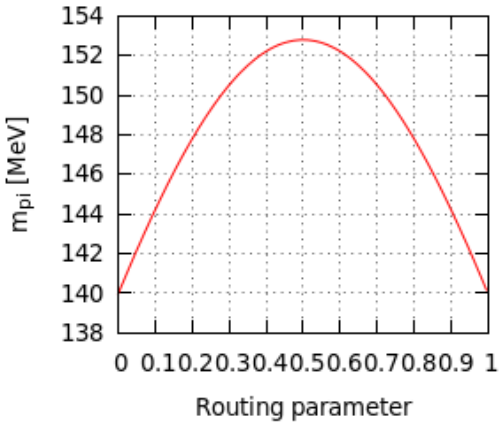

(a) The pion mass under variation of the routing parameter η for $m_c = 7.8\,\mathrm{MeV}$. The curve shows parabolic behaviour within an error margin of about 0.5%.

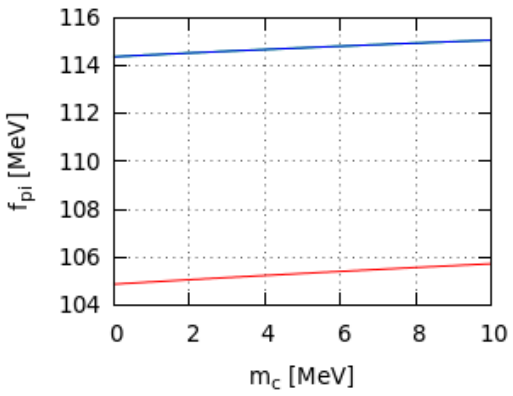

(b) Using the hard cutoff the decay constant depends on the routing parameter. The upper graphs is for symmetric, the lower for antisymmetric routing.

Figure 3.5: *Left panel:* The pion mass as a function of η. *Right panel:* The leptonic decay constant as a function of m_c in both momentum routings.

determine m_π as a function of m_c have been repeated with the new regulators. The results are plotted in figure 3.6b. With the changed method of regularization, the mass becomes independent of the momentum routing. It does also not change the results, which of the two quark propagators is being regularized.

In the chiral limit the pions indeed have zero mass, as Goldstone's theorem predicted. For small quark masses the mass of the pion increases harshly and it continues to increase for higher quark masses. We can see, that the mass of the pion outweighs the constituents mass by more then a factor of 18 for high current quark masses. Close to the chiral limit this factor is even bigger. The experimental value for the mass of a charged pion, about 140 MeV, is obtained for a quark mass of $m_c = 5.92\,\mathrm{MeV}$. This is not equal to the well known experimental values for the u and d quarks, but this can be seen as a result of the simplifications made in section 2.6. The quantities we use in the equations should be chosen to reconstruct the experimental values. If we were to consider a more general approach to the theory with less simplifications, it is possible to get closer to the experimental values [3].

Another interesting thing to look at is the behaviour of the pions under a varying interaction strength. Since pions are a bound state of a quark-antiquark pair held together by the strong interaction, it seems natural to expect its properties to change if the coupling strength changes too. To test this hypothesis we calculated the pion's mass for various m_G^{-2} up to a value of $61\,\mathrm{GeV}^{-2}$. The results are

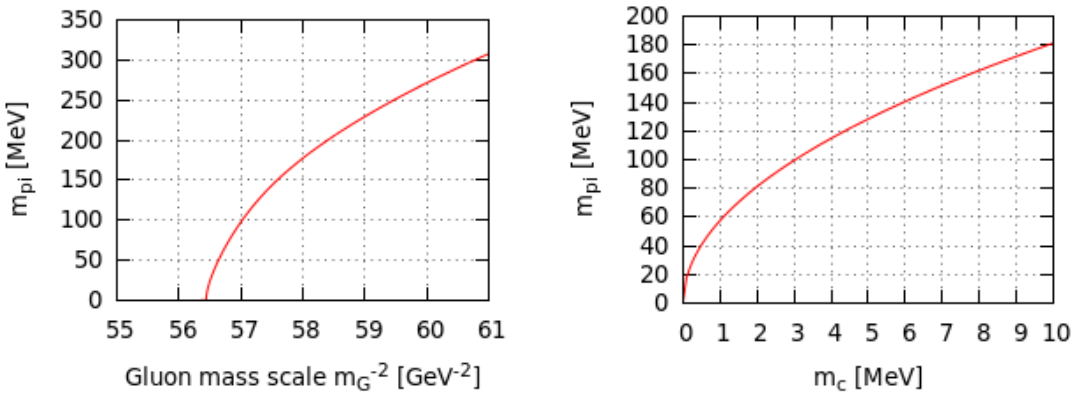

(a) We only find a solution for m_π for for $m_G \lesssim 133.1\,\text{MeV}$, for higher values of the interaction strength the pion mass quickly increases.

(b) $m_\pi(m_c)$ with the alternative regularization. The resulting pion mass is independent of the routing used. It does not matter, which propagator is regularized.

Figure 3.6: *Left panel:* The pion mass as a function of m_G^{-2}. *Right panel:* The pion mass as a function of m_c using the exponential regularization method.

shown in figure 3.6a For small values of m_G^{-2}, or equivalently large values of m_G, no solution can be found for m_π. This means, that only for a quark gluon mass scale of $m_G \lesssim 133.1\,\text{MeV}$ pions can form. Interestingly, this is beyond the point of spontaneous breaking of chiral symmetry we found in section 3.1.2. This means that pions occur only while a quark condensate is present in the QCD vacuum. As soon as that critical value of the gluon mass scale is surpassed, the mass of the pion increases rapidly. This happens since the binding energy of the quarks increases and due to the equivalence of energy and mass, the pions mass increases consequently.

Now that we calculated the correct pion mass, the BSE can be solved. If we use the hard cutoff for regularization, we will again end up with results depending on the chosen routing, as figure 3.5b shows. Therefore we will again be using the alternative regulators. Evaluating equation (3.18) with the exponential regularization gives us a ratio between the amplitudes of $\alpha = 0.11252$. From this result we can already derive, that E will be the leading amplitude that mainly defines the physical properties. Taking the canonical normalization condition (2.44) into account,[7] we get the normalized amplitudes

[7]The derivative in the normalization condition has been taken numerically with $\varepsilon = 10^{-6}$.

$$E = 3.898 \tag{3.20}$$

$$F = 0.439. \tag{3.21}$$

With these results we obtain a leptonic decay constant of

$$f_\pi = 93.76\,\mathrm{MeV}. \tag{3.22}$$

Instead of calculating f_π explicitly, it is also possible to consult the Gell-Mann-Oakes-Renner relation (2.28) to calculate f_π. Using our results for m_c, m_π and $\langle \overline{Q}Q \rangle$, the GMOR relation results in $f_\pi^{\mathrm{GMOR}} = 91.67\,\mathrm{MeV}$, which only deviates from the explicit result by about 2.2%.

Chapter 4

Pion in a moving frame

The calculations done up to this point already have been done in previous theses with similar results [15]. The following chapter contains investigations of the contact interaction model in a moving frame of reference, which in this form, have not been done yet.

4.1 Mathematical approach

Since the Bethe-Salpeter equation can be derived entirely from the covariant formulation of QCD, the BSE is fully covariant, too. As a consequence the Bethe-Salpeter amplitude Γ^μ transforms like a four-vector. This means that the amplitude in a moving frame Σ' is given by

$$(\Gamma')^\mu = \Lambda^\mu{}_\nu \Gamma^\nu, \tag{4.1}$$

where Λ is an element of the group of Lorentz transformations. Since all Lorentz transformations satisfy the identity[1]

$$g = \Lambda \cdot g \cdot \Lambda^T, \tag{4.2}$$

the scalar product of two four-vectors is invariant under Lorentz transformations

$$a'_\mu b'^\mu = g_{\mu\nu} a'^\nu b'^\mu = \Lambda_{\rho\mu} g_{\mu\nu} \left(\Lambda^T\right)_{\nu\sigma} a^\rho b^\sigma = g_{\rho\sigma} a^\rho b^\sigma = a_\sigma b^\sigma. \tag{4.3}$$

[1] Using the criteria for subgroups it is possible to show that all transformations satisfying this identity do indeed form a group.

Combining this with the pion's on-shell condition $P_\mu P^\mu = -m_\pi^2$ we see that the mass of the pion is Lorentz invariant. Our goal is to test, if this actually holds true in our model with the contact interaction (2.50). We do this by simply boosting the momentum four-vector $P^\mu = (im_\pi, 0, 0, 0)$ along the P_1 axis

$$P^\mu \longrightarrow P'^\mu = \left(i\sqrt{m_\pi^2 + P_1^2}, P_1, 0, 0 \right). \tag{4.4}$$

The boosted momentum still satisfies the on-shell condition[2] $P^2 = -m_\pi^2$. When we plug this new momentum into the Bethe-Salpeter equation, most calculations stay the same. The only thing that changes are the scalar products between the total momentum four-vector P and the four-vector of the inner momentum, that is integrated over. Those will contain an additional angular dependence which will cause the integrals in the elements of the κ-matrix to become three dimensional instead of two dimensional. So the full integrals given in equation (3.12) have to be solved. In particular the scalar product becomes

$$\begin{aligned} q \cdot P =& iq\sqrt{m_\pi^2 + P_1^2}\cos\psi + qP_1 \sin\psi \cos\vartheta \\ =& iqz\sqrt{m_\pi^2 + P_1^2} + qP_1 y\sqrt{1-z^2}, \end{aligned}$$

with the abbreviations $z = \cos\psi$ and $y = \cos\vartheta$ used for the angular coordinates, which have been introduced in section A.4 of the appendix.

4.2 Numerical results

The first thing we will test is how the mass of the pion behaves under Lorentz transformation. The calculation has been done analogous to the rest frame case with the difference of one additional variable, P_1, that has to be taken into account. Again, both methods of regularization have been applied to the integrals in the κ-matrix.

Using the hard cutoff we calculated m_π as a function of the three-momentum up to a value of $P_1 = 362\,\text{MeV}$. The results are shown in figure 4.1. One can see that for momenta up to about 342 MeV the mass is invariant, as we expected. For higher momenta the calculated mass harshly increases. This behaviour continues up to a momentum of 362 MeV, over which no meaningful results can be obtained.

[2]For convenience the prime at P' is suppressed from now on when it is clear that we are working in the moving frame.

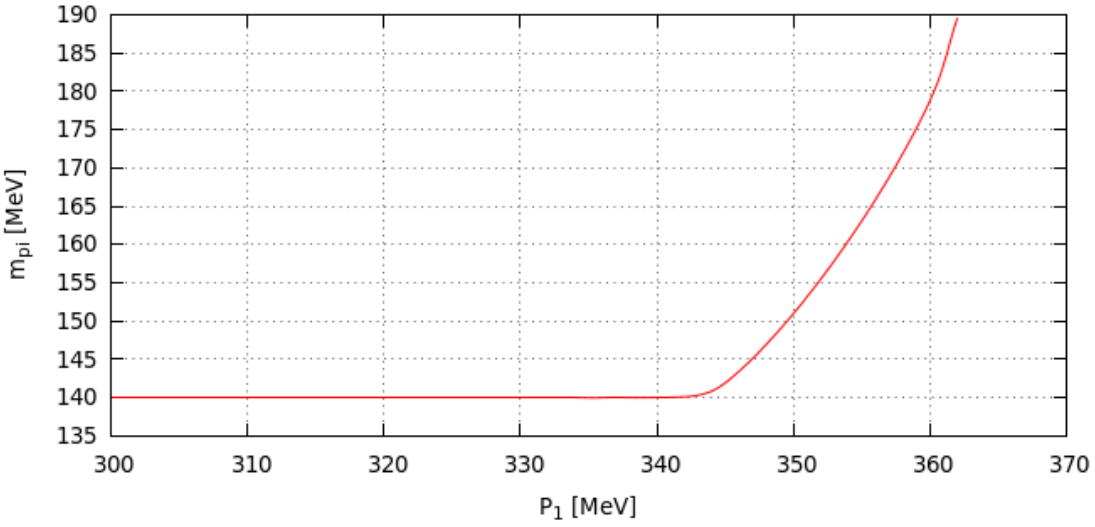

Figure 4.1: The pion mass as a function of P_1 in antisymmetric routing. For momenta over 362 MeV no meaningful solution can be found. For momenta under 342 MeV the mass is constant.

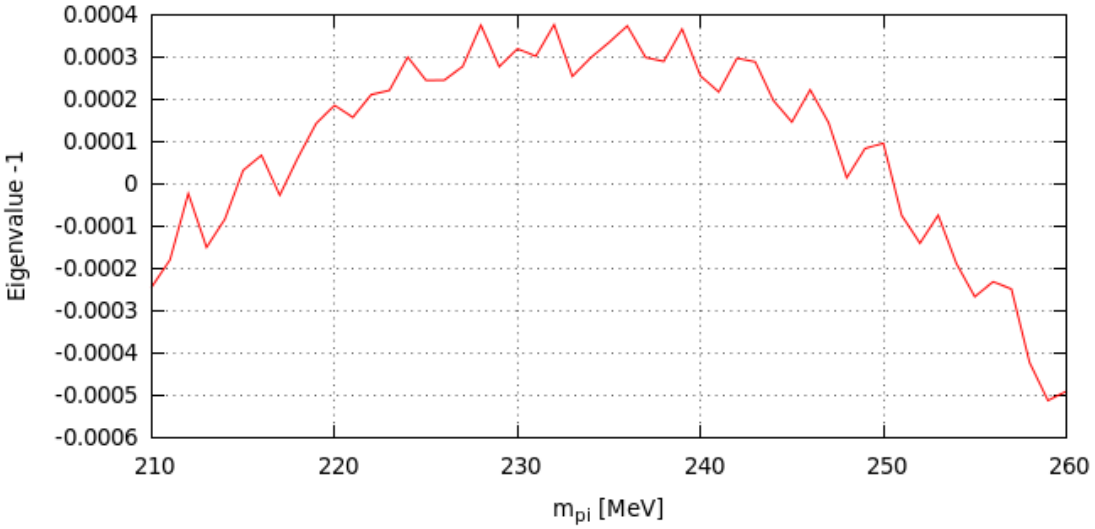

Figure 4.2: $\lambda - 1$ as a function of m_π at a momentum of $P_1 = 360\,\text{MeV}$. Within the interval $m_\pi \in [210, 260]\,\text{MeV}$ four different zeros can be found up to 36 MeV apart.

To investigate where this, obviously nonphysical behaviour, stems from, we take a look at the behaviour of the eigenvalue occurring in the BSE. Figure 4.2 show the typical behaviour of eigenvalue after subtracting one for a varying pion mass calculated at a momentum beyond 362 MeV. In the rest frame this function has one root at the physical mass. At high momenta the curve starts fluctuating heavily and crosses the m_π axis four times. This would mean that four different masses can be found which lead to an eigenvalue of 1. Since the mass can only have one value, it is not possible to draw any physical results from the calculations.

Trying to calculate the amplitudes with the hard cutoff does not result in good results either. The ratio α shows similar behaviour as the mass, as seen in figure 4.3a. This result means that the ratio between the amplitudes does not change for momenta up to $P_1 \simeq 340\,\text{MeV}$. After that point the significance of the amplitude E increases harshly until again no meaningful results can be calculated for $P_1 \gtrsim 362\,\text{MeV}$. When taking the normalization of the amplitude into account, the significance of the results for high momenta become more questionable. The results for the amplitudes E and F are shown in figure 4.3b. Their behaviour for high momenta does not show any clear pattern. As a result, calculating the leptonic decay constant from these amplitudes leads to similarly chaotic results. This clearly is a nonphysical result, as the decay constant should not show such behaviour but rather be Lorentz invariant as well.

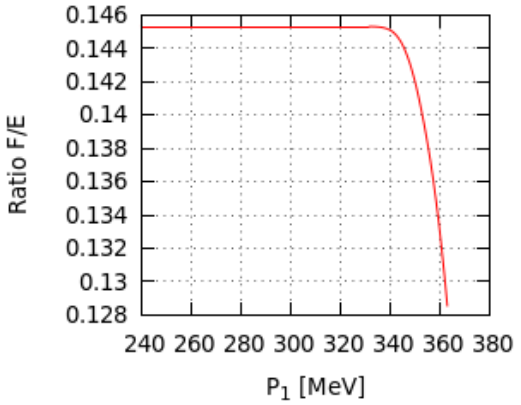

(a) For high momenta the ratio drops, meaning that E becomes even more significant.

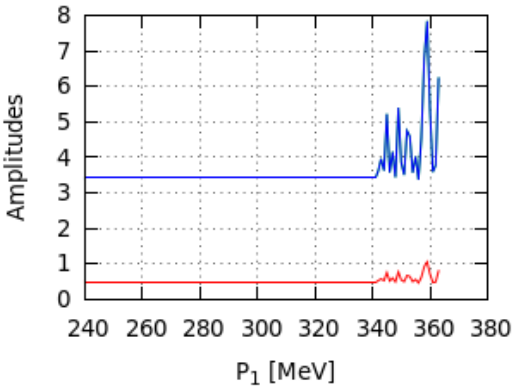

(b) Both amplitudes E (upper graph) and F (lower graph) show no obvious predictable behaviour at high momenta.

Figure 4.3: Results for the BSA using the hard ultraviolet cutoff calculated in antisymetric momentum routing. *Left panel:* The ratio $\alpha = F/E$ as a function of P_1. *Right panel:* The normalized amplitudes E and F as a function of P_1.

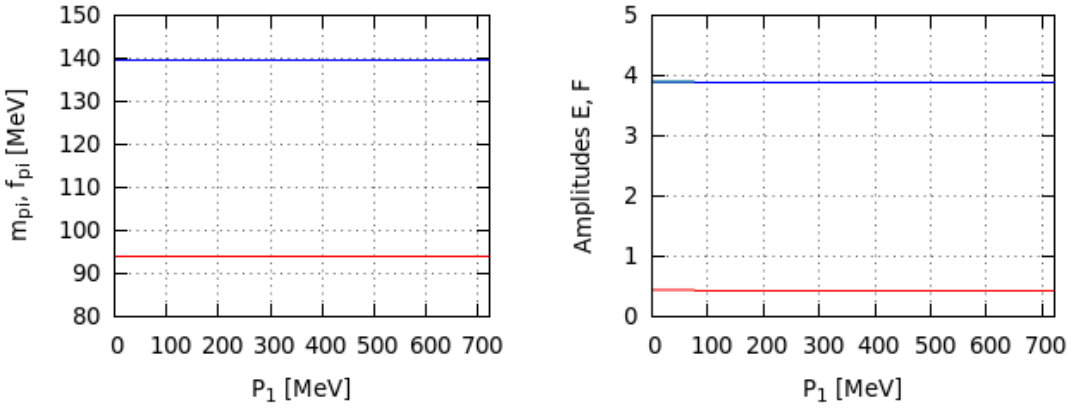

(a) The mass m_π (upper graph) and the leptonic decay constant f_π (lower graph).

(b) The Amplitudes E (upper graph) and F (lower graph).

Figure 4.4: Behaviour of the pion's properties under Lorentz transformation calculated using the exponential regularization. The properties stay invariant even for high momenta.

As a conclusion we conduct that the contact interaction model fails to give suitable results for high momenta, or equivalently high energies, when regularized by the hard cutoff parameter.

The next logical step is to test, how well the model is able to describe high momentum pions when the alternative approach to regularization is consulted. For the mass of the pion, the results using the alternative regularization do not have the problems of the hard cutoff. We are able to calculate the mass for way higher momenta more consistently. For momenta over $\sim 725\,\mathrm{MeV}$ the problem becomes more of a challenge to the numerical methods used, but this does not manifest in the results they produce.

The remaining properties of the pion are also found to be Lorentz invariant. Both amplitudes (E, F) and the leptonic decay constant f_π remain constant for high momenta. This is what we expected and suits the real behaviour of physical particle better then the results obtained with the hard cutoff.

Chapter 5

Conclusion and Outlook

In this thesis we saw that even simple models like the contact interaction can be used to reproduce appropriate results for the physical properties of the lightest quarks and mesons. We have also seen that seemingly minor changes, such as changing the method of regularization used, are highly non trivial and might lead to completely different behaviour. This can be seen in the calculation of the mass of the pion, where the hard cutoff approach to regularization produced results that still depended on the momentum routing which should not influence the physics at all. When we solved the BSE in the moving frame this discrepancy manifested even further with the hard cutoff approach violating fundamental principles like the Lorentz invariance of the pion's mass.

When we introduced the Rainbow-Ladder truncation in addition to the contact interaction we assumed the gluon propagator and therefore the coupling strength $\alpha(k^2)$ to be constant. To obtain even better results one should use the full gluon propagator in Rainbow-Ladder truncation [8]

$$D^{\mu\nu}(k) = \frac{Z(k^2)}{k^2}\left(\delta^{\mu\nu} - \frac{k^\mu k^\nu}{k^2}\right), \tag{5.1}$$

introducing another dressing function $Z(k^2)$. Furthermore the quark-gluon vertex can be dressed too via

$$\Gamma_\mu = \gamma_\mu \Gamma(k^2), \tag{5.2}$$

with yet another dressing function $\Gamma(k^2)$. These dressing functions are usually combined to get

$$\alpha(k^2) \equiv \frac{g^2}{4\pi} Z(k^2) \cdot \Gamma(k^2). \tag{5.3}$$

Quantity	**This thesis**	**Maris-Tandy model**	**Experiment**
$m_{u/d}$	5.92	3.74	2.5 – 5.5
m_π	139.6	140	139.6
f_π	93.8	91.7	92.1

Table 5.1: Comparison between the results of this thesis, results for a more accurate model taken from [9] and experimental values taken from [1] and [16].

As tab. 5.1 shows, it is possible to get very close to the measured values using the enhanced model. It is also possible to go beyond the Rainbow-Ladder truncation by using lattice QCD methods.

The calculations done in the moving frame might seem trivial at first glance, but indeed have their applications in recent research. Similar calculations are done for instance to investigate electromagnetic form factors [17]. Another approach to the moving frame solutions of the BSE is by using a Green's function approach to investigate the movement of the energy-plane poles of the Green's function [18].

We conclude that even simple models like the contact interaction model are able to describe the physics of the lightest quarks and mesons properly even in a moving frame of reference for reasonable high momenta, compared to the mass of the particles involved. The numerical methods might need some refinement at a certain point when solving the equations for high momenta to still yield reasonable results.

Appendix A

Conventions and relations

A.1 Euclidean conventions

In all of the calculations in this thesis Euclidean conventions are applied, which means that the used metric is given by

$$g_{\mu\nu} = g_{\mu}{}^{\nu} = g^{\mu\nu} = \begin{pmatrix} 1 & 0 & 0 & 0 \\ 0 & 1 & 0 & 0 \\ 0 & 0 & 1 & 0 \\ 0 & 0 & 0 & 1 \end{pmatrix}. \tag{A.1}$$

With that, scalar products of four vectors can be written as

$$a \cdot b = \sum_{\mu=0}^{3} a_\mu b_\mu \equiv a_\mu b^\mu = a^\mu b_\mu. \tag{A.2}$$

Associated with the use of an Euclidean instead of a Minkowski metric the four momentum vector has been Wick rotated, such that

$$p^\mu := \begin{pmatrix} iE \\ \vec{p} \end{pmatrix}, \tag{A.3}$$

where $E = \sqrt{m^2 + |\vec{p}|^2}$ is the Energy and $\vec{p}$ is the three momentum vector. In this convention, a four vector $p \in \mathbb{C} \times \mathbb{R}^3$ is spacelike, if $p^2 > 0$.

A.2 Gamma matrices

The gamma matrices γ_μ ($\mu \in \{0,1,2,3,5\}$), also sometimes called Dirac matrices, are a set of matrices, that obey a certain (anti-)commutator algebra. One possible representation of the matrices in Euclidean convention is via the Pauli matrices $\vec{\sigma}$:

$$\gamma_0 = \begin{pmatrix} \mathbb{1} & 0 \\ 0 & -\mathbb{1} \end{pmatrix}, \quad \gamma_j = \begin{pmatrix} 0 & i\sigma_j \\ -i\sigma_j & 0 \end{pmatrix}, \quad \gamma_5 = \begin{pmatrix} 0 & \mathbb{1} \\ \mathbb{1} & 0 \end{pmatrix}, \tag{A.4}$$

where $\mathbb{1} = \mathbb{1}_{2\times 2}$ and $j \in \{1,2,3\}$. In Euclidean metric the gamma matrices are hermitian

$$\gamma_\mu = (\gamma_\mu)^\dagger \tag{A.5}$$

and obey the anticommutator rules of a Clifford algebra

$$[\gamma_\mu, \gamma_\nu]_+ = 2\delta_{\mu\nu}. \tag{A.6}$$

Helpful relations

In some derivations in this thesis traces of products of gamma matrices are evaluated. Therefore the following relations for products and traces of gamma matrices are used frequently.

Products:

- $(\gamma_5)^2 = \mathbb{1}$
- $[\gamma_\mu, \gamma_\nu]_+ = 2\delta_{\mu\nu}$
- $\gamma_j \gamma^j = 4 \cdot \mathbb{1}$
- $\gamma_\mu \gamma_\nu \gamma^\mu = -2\gamma_\nu$
- $\gamma_\mu \gamma_\nu \gamma_\rho \gamma^\mu = 4\delta_{\nu\rho} \cdot \mathbb{1}$
- $\gamma_\mu \gamma_\nu \gamma_\rho \gamma_\sigma \gamma^\mu = -2\gamma_\sigma \gamma_\rho \gamma_\nu$

Here again j and μ can take the value $\{1,2,3\}$ and $\{0,1,2,3\}$ respectively. Additionally, the anticommutator of γ_5 and every other gamma matrix vanishes.

Traces:

- $\mathrm{tr}(\gamma_\mu) = 0$
- $\mathrm{tr}(\gamma_\mu \gamma^\mu) = 16$
- $\mathrm{tr}(\gamma_\mu \gamma_\nu) = 4\delta_{\mu\nu}$
- $\mathrm{tr}(\gamma_\mu \gamma_\nu \gamma_\rho \gamma_\sigma) = 4(\delta_{\mu\nu}\delta_{\rho\sigma} + \delta_{\mu\sigma}\delta_{\nu\rho} - \delta_{\mu\rho}\delta_{\nu\sigma})$
- $\mathrm{tr}(\underbrace{\gamma_\alpha \gamma_\beta \dots \gamma_\omega}_{\text{odd\#}}) = 0$

A.3 Natural units

All equations and results in this thesis are calculated in a natural unit system. In this system we use the fact, that the speed of light c and the Planck constant $\hbar$ are finite value greater than zero, but the physics don't change qualitatively if they are exchanged for another value. So for convenience we set them to $\hbar = c = 1$. This also leads to the convenient situation that only powers of one unit, the unit of energy, are required to describe physical quantities. Some important examples for that are given in table A.1. When converting back to SI units it is sufficient to multiply the value in natural units by a conversion factor, which is a power of $\hbar$ and c in SI units. For example to convert a distance x given in natural units to SI units, it needs to be multiplied by a factor of $\hbar c = 197.327\,\mathrm{MeV\,fm}$ to be given in terms of meters.

Quantity	SI	N.u.	Conversion factor
Energy	J	eV^1	1
Momentum	$\mathrm{kg\,m\,s^{-1}}$	eV^1	c^{-1}
Mass	kg	eV^1	c^{-2}
Time	s	eV^{-1}	$\hbar$
Length	m	eV^{-1}	$\hbar c$
Energy density	$\mathrm{J\,m^{-3}}$	eV^4	$(\hbar c)^{-3}$

Table A.1: Natural and SI units for some important quantities and the corresponding conversion factor f, such that $A_{SI} = f A_{n.u.}$

A.4 Feynman slash notation

Another practical abbreviation is the so called Feynman slash notation. It stands for a scalar product between a four vector and a vector containing the gamma matrices γ_0 to γ_3,

$$\not{A} := \gamma_\mu A^\mu. \tag{A.7}$$

Due to the fact, that the gamma matrices' trace is zero, the trace of every slashed vector is zero as well.

$$\mathrm{tr}(\not{A}) = 0 \tag{A.8}$$

Since the gamma matrices form a Clifford algebra, see eqn. (A.6), the scalar product of two slashed vectors is invariant

$$\not{A} \cdot \not{B} = (A \cdot B) \cdot \mathbb{1}_{4\times 4}. \tag{A.9}$$

A.5 Integration in hyperspherical coordinates

Throughout this thesis there are several four-dimensional integrals to calculate. For convenience they have been evaluated in hyperspherical coordinates, which are a generalization of three-dimensional spherical coordinates. A general, four-dimensional vector $x = (x_0, x_1, x_2, x_3)$ can be expressed as

$$x_0 = r\cos\psi \tag{A.10}$$
$$x_1 = r\sin\psi\cos\vartheta \tag{A.11}$$
$$x_2 = r\sin\psi\sin\vartheta\cos\varphi \tag{A.12}$$
$$x_3 = r\sin\psi\sin\vartheta\sin\varphi \tag{A.13}$$

Using this convention the Jacobi-determinant becomes

$$\mathrm{d}^4x = \mathrm{d}\varphi\mathrm{d}\vartheta\sin\vartheta\mathrm{d}\psi\sin^2\psi\mathrm{d}r r^3, \tag{A.14}$$

so that the integral of a function of x can be rewritten as

$$\int_{\mathbb{R}^4} f(x)\mathrm{d}^4x = \int_0^{2\pi} \mathrm{d}\varphi \int_0^{\pi} \mathrm{d}\vartheta \sin\vartheta \int_0^{\pi} \mathrm{d}\psi \sin^2\psi \int_0^{\infty} \mathrm{d}r r^3 f(r,\psi,\vartheta,\varphi). \tag{A.15}$$

Introducing the abbreviations $y = \cos\vartheta$ and $z = \cos\psi$ we can express eq. (A.15) in terms of z and y

$$\int_{\mathbb{R}^4} f(x)\mathrm{d}^4x = \int_0^{2\pi} \mathrm{d}\varphi \int_{-1}^{1} \mathrm{d}y \int_{-1}^{1} \mathrm{d}z\sqrt{1-z^2} \int_0^{\infty} \mathrm{d}r r^3 f(r,z,y,\varphi). \tag{A.16}$$

In most equations in this thesis the function which is integrated over only depends on two or three variables, so we further use the abbreviations

$$\int^{\Lambda} \mathrm{d}(r,z,y) \quad \to \quad \int_{-1}^{1} \mathrm{d}y \int_{-1}^{1} \mathrm{d}z\sqrt{1-z^2} \int_0^{\Lambda} \mathrm{d}r r^3 \tag{A.17}$$

$$\int^{\Lambda} \mathrm{d}(r,z) \quad \to \quad \int_{-1}^{1} \mathrm{d}z\sqrt{1-z^2} \int_0^{\Lambda} \mathrm{d}r r^3 \tag{A.18}$$

Appendix B

Derivations

B.1 Proof of Goldstone's theorem

Consider a theory involving multiple scalar fields $\phi^a(x)$ and a Lagrangian of the form

$$\mathcal{L}(\partial\phi, \phi) = T(\partial\phi) - V(\phi), \tag{B.1}$$

where T only depends on derivatives of the field and V only on the field itself. Let ϕ_0^a be a constant field, which minimizes V, such that

$$\frac{\partial}{\partial\phi^a} V \bigg|_{\phi^a=\phi_0^a} = 0 \tag{B.2}$$

If we calculate the Taylor expansion of V around ϕ_0^a up to the second order, we get

$$V(\phi) = V(\phi_0) + \frac{1}{2}(\phi-\phi_0)^a(\phi-\phi_0)^b \left(\frac{\partial^2}{\partial\phi^a\partial\phi^b} V\right)_{\phi=\phi_0}. \tag{B.3}$$

Note, that the linear term in the expansion vanishes, since its coefficient is identical to the left hand side of eq. (B.2). Since ϕ_0 is a minimum of V, the coefficients of the quadratic term have to be greater or equal to zero. We can identify them as the eigenvalues of a square matrix, which can be interpreted as the masses of the fields

$$m_{ab}^2 := \left(\frac{\partial^2}{\partial\phi^a\partial\phi^b} V\right)_{\phi=\phi_0} \geq 0. \tag{B.4}$$

To proof Goldstone's Theorem, we have to show, that every spontaneously broken continuous symmetry, i.e. every continuous symmetry of the Lagrangian, that is not a symmetry of ϕ_0, yields an eigenvalue of the mass matrix, that is equal to zero. To do that, we start with a general, continuous symmetry transformation of the form

$$\phi^a \to \phi^a + \varepsilon\Delta^a(\phi), \tag{B.5}$$

where ε is an infinitesimal parameter and $\Delta^a(\phi)$ is a function, that depends on all of the fields. If we assume constant fields, all of the derivatives in the Lagrangian vanish and only V has to be invariant under this transformation. If we apply the transformation, we get

$$V(\phi^a) \stackrel{!}{=} V(\phi^a + \varepsilon\Delta^a(\phi)), \tag{B.6}$$

which is equivalent to

$$V(\phi^a + \varepsilon\Delta^a(\phi)) - V(\phi^a) \equiv \varepsilon\Delta^a(\phi)\frac{\partial}{\partial\phi^a}V(\phi) = 0. \tag{B.7}$$

In the last step we used the fact that ε is an infinitesimal parameter, which lead to the derivative of V. If we now divide this equation by ε, differentiate with respect to ϕ^b and evaluate the result at $\phi = \phi_0$, we get

$$\frac{\partial}{\partial\phi^b}\left(\Delta^a\frac{\partial V}{\partial\phi^a}\right)_{\phi_0} = \left(\frac{\partial\Delta^a}{\partial\phi^b}\right)_{\phi_0}\left(\frac{\partial V}{\partial\phi^a}\right)_{\phi_0} + \Delta^a(\phi_0)\cdot m^2_{ab} = 0. \tag{B.8}$$

Again, using eq. (B.2) we see, that the first term in this equation vanishes. Consequently, the second expression has to be zero as well and since we did not apply any further conditions to Δ^a, m_{ab} has to be zero as well. With that, Goldstone's Theorem is proven. For a more general proof of the theorem and additional explanations, [19] can be consulted.

B.2 Derivation of the gap equation

B.2.1 Derivation of the general form

To derive the gap equation, we start with the quark DSE

$$S(p) = S_0(p) + S_0(p)\Sigma(p)S(p). \tag{B.9}$$

If we iterate this equation we get the infinite series

$$\begin{aligned} S(p) =& S_0(p) + S_0(p)\Sigma(p)S_0(p) + S_0(p)\Sigma(p)S_0(p)\Sigma(p)S_0(p) + \dots \\ =& S_0(p)\left(\sum_{i=0}^{\infty}\left(\Sigma(p)S_0(p)\right)^i\right) \\ =& S_0(p)\frac{1}{1-\Sigma(p)S_0(p)}. \end{aligned}$$

In the last step we assumed the series to converge, so that we can apply the formula for a geometric series. If we now take the inverse of both sides of the equation, we end up with the desired equation

$$S^{-1}(p) = \left(1-\Sigma(p)S_0(p)\right)S_0^{-1}(p) = S_0^{-1}(p) - \Sigma(p). \tag{B.10}$$

B.2.2 Calculation of the dressing functions

First, we want to calculate the function $A(p^2)$. To do this, we multiply eq. (3.2) with $-i\not{p}$ from the left to obtain

$$p^2A(p^2) - i\not{p}B(p^2) = p^2 - im_c\not{p} - \frac{4}{3m_G^2}\int\frac{\mathrm{d}^4q}{(2\pi)^4}\gamma_\mu\frac{\not{p}\not{q}A(q^2)+i\not{p}B(q^2)}{q^2A^2(q^2)+B^2(q^2)}\gamma^\mu. \tag{B.11}$$

Taking the trace of this equation, all terms with an odd number of gamma matrices vanish, so we are left with

$$4p^2A(p^2) = 4p^2 - 16\frac{4}{3m_G^2}\int\frac{\mathrm{d}^4q}{(2\pi)^4}\frac{(p_\mu q^\mu)A(p^2)}{q^2A^2(q^2)+B^2(q^2)}. \tag{B.12}$$

We can explicitly evaluate the scalar product $(p_\mu q^\mu)$ by aligning the x_0 axis of the coordinate system of q with the direction of p. With that choice of coordinates,

it can be expressed as $p_\mu q^\mu = pq\cos\psi$, where ψ is the angle introduced in section A.4. Together with the functional determinant, the integral in above equation contains the term

$$\int_0^\pi \mathrm{d}\psi \sin^2\psi\cos\psi = 0. \tag{B.13}$$

Hence the full integral is equal to zero, so that we are left with

$$4p^2A(p^2) = 4p^2 \qquad \Longleftrightarrow \qquad A(p^2) \equiv 1. \tag{B.14}$$

With this result the effective quark mass M is equal to the second dressing function $B(p^2)$, so they will be used interchangeably. To calculate M, we start by directly taking the trace of eq. (3.2):

$$4M = 4m_c + 16\frac{4}{3m_G^2}\int \frac{\mathrm{d}^4q}{(2\pi)^4}\frac{M}{q^2+M^2} \tag{B.15}$$

Dividing this equation by 4 results in an iterative equation for M. Since the integral on the right-hand-side of this equation only depends on q and none of the hyperspherical angles, the integration can be done trivially in three dimensions, giving a factor of $2\pi^2$. Additionally the integrated function only depends on q^2, so we conveniently introduce the substitution

$$\int \mathrm{d}q\cdot q^3 \quad \longrightarrow \quad \frac{1}{2}\int \mathrm{d}(q^2)\cdot q^2 \equiv \frac{1}{2}\int \mathrm{d}s\cdot s.$$

After all, we end up with the final equation

$$M = m_c + \frac{1}{3m_G^2\pi^2}\int_0^\infty \mathrm{d}s\frac{sM}{s+M^2}. \tag{B.16}$$

B.3 Derivation of the Bethe-Salpeter equation

B.3.1 Derivation of the general form

To begin with, we introduce the convenient abbreviations

$$\widetilde{T} := TG_0, \qquad \widetilde{K} := KG_0. \tag{B.17}$$

Using the fact, that T obeys the Dyson equation, we can rewrite $\widetilde{T}$ as

$$\begin{aligned}
\widetilde{T} =& TG_0 = (K + KG_0T)\, G_0 && \text{(B.18)}\\
=& KG_0 + KG_0KG_0 + KG_0KG_0KG_0 + \dots && \text{(B.19)}\\
=& \widetilde{K}\left(\sum_{n=0}^{\infty}\left(\widetilde{K}\right)^n\right) && \text{(B.20)}\\
=& \widetilde{K}\frac{1}{1-\widetilde{K}}. && \text{(B.21)}
\end{aligned}$$

Multiplying this equation with $(1 - \widetilde{K})$ from the left yields

$$\widetilde{K} = \left(1 - \widetilde{K}\right)\widetilde{T} = \widetilde{T} - \widetilde{K}\widetilde{T}, \tag{B.22}$$

which is equivalent to

$$\widetilde{T} = \widetilde{K} + \widetilde{K}\widetilde{T} = \widetilde{K}\left(1 + \widetilde{T}\right). \tag{B.23}$$

If we now use our ansatz for T with a proportionality constant $\mathcal{N}$, we get

$$\begin{aligned}
\mathcal{N}\frac{\Gamma\overline{\Gamma}}{P^2+m^2}G_0 =& KG_0\left(1 + \mathcal{N}\frac{\Gamma\overline{\Gamma}}{P^2+m^2}G_0\right) && \text{(B.24)}\\
=& \left(K + KG_0\mathcal{N}\frac{\Gamma\overline{\Gamma}}{P^2+m^2}\right)G_0 && \text{(B.25)}\\
=& \frac{1}{P^2+m^2}\left(KG_0\mathcal{N}\Gamma\overline{\Gamma}\right). && \text{(B.26)}
\end{aligned}$$

In the last step we have used the fact, that for on shell particles $P^2 = -m^2$. Comparing the left-hand-side of the equation with the right-hand-side, we obtain our desired result

$$\Gamma\overline{\Gamma} = KG_0\Gamma\overline{\Gamma} \quad \Longleftrightarrow \quad \Gamma = KG_0\Gamma \tag{B.27}$$

B.3.2 Derivation of the truncated form

To derive the matrix elements of the 2×2 matrix, we again start by using the handy abbreviations

$$a := -\frac{4}{3m_G^2}, \qquad b^{-1} := (q_-^2 + M^2)(q_+^2 + M^2) \tag{B.28}$$

Plugging the Dirac composition of the BSA into the equation (2.52), we get

$$\gamma^5(iE + \frac{\not{P}}{M}F) = a\int \frac{\mathrm{d}^4q}{(2\pi)^4} b\gamma_\mu(M - i\not{q}_+)\gamma^5(iE + \frac{\not{P}}{M}F)(M - i\not{q}_-)\gamma^\mu$$

To deal with the gamma matrices, we explicitly write every slashed four-vector out and group the gamma matrices together. Doing so we get the expression

$$\begin{aligned} a\int \frac{\mathrm{d}^4q}{(2\pi)^4} b\{&E[(\gamma_\mu\gamma_\alpha\gamma^5\gamma^\mu)Mq_+^\alpha - i(\gamma_\mu\gamma_\alpha\gamma^5\gamma_\nu\gamma^\mu)q_+^\alpha q_-^\nu + (\gamma_\mu\gamma^5\gamma_\nu\gamma^\mu)Mq_-^\nu \\ &+i(\gamma_\mu\gamma^5\gamma^\mu)M^2] + F[(\gamma_\mu\gamma^5\gamma_\beta\gamma^\mu)MP^\beta - (\gamma_\mu\gamma_\alpha\gamma^5\gamma_\beta\gamma_\nu\gamma^\mu)q_+^\alpha q_-^\nu P^\beta M^{-1} \\ &-i(\gamma_\mu\gamma^5\gamma_\beta\gamma_\nu\gamma^\mu)q_-^\nu P^\beta - i(\gamma_\mu\gamma_\alpha\gamma^5\gamma_\beta\gamma^\mu)q_+^\alpha P^\beta]\} = \gamma^5(iE + \gamma_\beta\frac{P^\beta}{M}F) \end{aligned}$$

In this lengthy equation we can isolate E by multiplying with γ^5/i and using the identities mentioned in section A.2.

$$\begin{aligned} E - i\not{P}F = a\int \frac{\mathrm{d}^4q}{(2\pi)^4}\frac{b}{i}\{&E[2\not{q}_-M - 2\not{q}_+M - 4i(q_+\cdot q_-) - 4iM^2] + F[2M\not{P} \\ &+4i(q_-\cdot P) - 4i(q_+\cdot P) + 2\gamma_\nu\gamma_\beta\gamma_\alpha q_+^\alpha q_-^\nu P^\beta M^{-1}] \end{aligned}$$

The last step is to take the trace of both sides of this equation and divide the result by 4, so that we get

$$E = 4a\int \frac{\mathrm{d}^4q}{(2\pi)^4} b\left(\left[-(q_-\cdot q_+) - M^2\right]E + \left[(q_-\cdot P) - (q_+\cdot P)\right]F\right). \tag{B.29}$$

To derive an analogous expression for F, we multiply the lengthy equation from the left with $-M\not{P}\gamma^5/m_\pi^2$ and use the relation $P^2 = -m_\pi^2$:

$$-a\int\frac{\mathrm{d}^4 1}{(2\pi)^4}\frac{bM}{m_\pi^2}\{E[(\gamma_\rho\gamma^5\gamma_\mu\gamma_\alpha\gamma^5\gamma^\mu)Mq_+^\alpha P^\rho+(\gamma_\rho\gamma^5\gamma_\mu\gamma^5\gamma_\nu\gamma^\mu)Mq_-^\nu P^\rho$$
$$+i(\gamma_\rho\gamma^5\gamma_\mu\gamma^5\gamma^\mu)M^2P^\rho-i(\gamma_\rho\gamma^5\gamma_\mu\gamma_\alpha\gamma^5\gamma_\nu\gamma^\mu)q_+^\alpha q_-^\nu P^\rho]$$
$$+F[-i(\gamma_\rho\gamma^5\gamma_\mu\gamma_\alpha\gamma^5\gamma_\beta\gamma^\mu)q_+^\alpha P^\beta P^\rho-(\gamma_\rho\gamma^5\gamma_\mu\gamma_\alpha\gamma^5\gamma_\beta\gamma_\nu\gamma^\mu)M^{-1}q_+^\alpha q_-^\nu P^\beta P^\rho$$
$$+(\gamma_\rho\gamma^5\gamma_\mu\gamma^5\gamma_\beta\gamma^\mu)MP^\beta P^\rho-i(\gamma_\rho\gamma^5\gamma_\mu\gamma^5\gamma_\beta\gamma_\nu\gamma^\mu)q_-^\nu P^\beta P^\rho]\}=\frac{-iM\not{P}}{m_\pi^2}E+F$$

In analogy to the derivation of the equation for E, we now take the trace and divide the result by 4. After cleaning up all the gamma matrices, we are left with:

$$F=a\int\frac{\mathrm{d}^4 q}{(2\pi)^4}b\{\frac{2M^2}{m_\pi^2}F[2M^2-\frac{2}{m_\pi^2}((q_+\cdot P)(q_-\cdot P)+m_\pi^2(q_+\cdot q_-))]$$
$$+E[(q_+\cdot P)-(q_-\cdot P)]\}$$

Finally we can further simplify the equations for E and F by using the fact that $(q_+\cdot P)-(q_-\cdot P)=P^2=-m_\pi^2$. Without loss of generality we can choose the three-momentum $\vec{p}$ of the pion to be aligned with the P_1 direction, so that its four-momentum is given by $P^\mu=(i\sqrt{m_\pi^2+P_1^2},P_1)$. With that the scalar products of the form $q\cdot P$ further simplify to

$$q\cdot P=iq\sqrt{m_\pi^2+P_x^2}\cos\psi+qP_1\sin\psi\cos\vartheta\equiv iqz\sqrt{m_\pi^2+P_1^2}+qP_1y\sqrt{1-z^2}$$

with the notation introduced in section A.4. Since non of the scalar products depend on the integration variable φ, we can already solve one integral trivially. Lastly we introduce the constant $\mathcal{N}=\frac{1}{6m_G^2\pi^3}$, so that we finally remain with the matrix elements

$$\kappa_{EE}=4\mathcal{N}\int^\infty\mathrm{d}(q,z,y)\frac{(q_+\cdot q_-)+M^2}{(q_-^2+M^2)(q_+^2+M^2)} \tag{B.30}$$
$$\kappa_{EF}=-4m_\pi^2\mathcal{N}\int^\infty\mathrm{d}(q,z,y)\frac{1}{(q_-^2+M^2)(q_+^2+M^2)} \tag{B.31}$$
$$\kappa_{FE}=2M^2\mathcal{N}\int^\infty\mathrm{d}(q,z,y)\frac{1}{(q_-^2+M^2)(q_+^2+M^2)} \tag{B.32}$$
$$\kappa_{FF}=-2\mathcal{N}\int^\infty\mathrm{d}(q,z,y)\frac{M^2-m_\pi^{-2}(m_\pi^2(q_+\cdot q_-)+2(q_+\cdot P)(q_-\cdot P))}{(q_-^2+M^2)(q_+^2+M^2)}. \tag{B.33}$$

B.4 Derivation of the chiral quark condensate

We start by substituting our result for the quark propagator into eq. (3.8)

$$\langle \overline{Q}Q \rangle = \mathcal{N} N_c \int \frac{\mathrm{d}^4 q}{(2\pi)^4} \,\mathrm{tr}\left(\frac{-i\not{q} + M}{q^2 + M^2} \right). \tag{B.34}$$

Again, using the tracelessness of the gamma matrices and evaluating the angular integrals, we get[1]

$$\langle \overline{Q}Q \rangle = \frac{3}{4\pi^2} \mathcal{N} \int_0^\infty \mathrm{d}x \frac{xM}{x + M^2}, \tag{B.35}$$

which also has to be regularized as well. Comparing this expression with equation (3.3), we can see, that $\langle \overline{Q}Q \rangle$ and M indeed satisfy the relation

$$\langle \overline{Q}Q \rangle / \mathcal{N} = \frac{9}{4} m_G^2 (M - m_c). \tag{B.36}$$

B.5 Derivation of the normalization condition

We start with equation (2.44):

$$1 = \frac{\mathrm{d}}{\mathrm{d}P^2} \,\mathrm{tr} \int \frac{\mathrm{d}^4 q}{(2\pi)^4} \overline{\Gamma}(q, K) S(q_+) \Gamma(q, K) S(q_-) \tag{B.37}$$

We plug in the expressions for Γ, $\overline{\Gamma}$ and S we obtained earlier

$$\Gamma = \gamma^5 \left(iE + \frac{\not{P}}{M} F \right), \quad \overline{\Gamma} = \gamma^5 \left(iE - \frac{\not{P}}{M} F \right), \quad S(q_\pm) = \frac{-i\not{q}_\pm + M}{q_\pm^2 + M^2}. \tag{B.38}$$

The following steps are analogous to the ones done in section B.3, so we will not do them as detailed here. Basically we write out the expressions in full and take the trace of colour, flavour and Dirac indices using the relations of the gamma matrices. After all of this is done, we can again integrate one of the four integrals trivially and end up with

[1] Assuming $N_c = 3$ for the three colors r, g, and b.

$$
\begin{aligned}
1 =& \frac{3}{\pi^3}\frac{\mathrm{d}}{\mathrm{d}P^2}\int \mathrm{d}(q,z,y)\Big\{[-M^2-(q_+\cdot q_-)]E^2-2(p\cdot K)EF \\
&+\left[K^2+M^{-2}(2(q_+\cdot K)(q_-\cdot K)-K^2(q_+\cdot q_-))\right]F^2\Big\} \\
&\cdot\left[(q_-^2+M^2)(q_+^2+M^2)\right]^{-1}.
\end{aligned}
$$

At this point it is possible to solve this equation by the method explained in section 3.2.1, but taking the derivative with respect to P^2 is rather unconventional. Thus we use the substitution

$$
\frac{\mathrm{d}}{\mathrm{d}P^2} \longrightarrow \frac{1}{2P}\frac{\mathrm{d}}{\mathrm{d}P} \tag{B.39}
$$

to achieve a differentiation with respect to P. After all we end up with the wanted relation

$$
\begin{aligned}
1 =& \frac{3}{2P\pi^3}\frac{\mathrm{d}}{\mathrm{d}P}\int \mathrm{d}(q,z,y)\Big\{[-M^2-(q_+\cdot q_-)]E^2-2(p\cdot K)EF \\
&+\left[K^2+M^{-2}(2(q_+\cdot K)(q_-\cdot K)-K^2(q_+\cdot q_-))\right]F^2\Big\} \\
&\cdot\left[(q_-^2+M^2)(q_+^2+M^2)\right]^{-1}.
\end{aligned}
$$

In the moving frame this equation has to be solved in full, while in the rest frame the integration over y can be done trivially, which yields a factor of 2.

Appendix C

Numerical methods and software used

Most of the equations in this thesis cannot be solved analytically, so numerical solution techniques have to be consulted. All of the computations have been programmed in C++11 using the JetBrains CLion IDE[1] and the C++ compiler from the GNU compiler collection, published under the GNU General Public License. The results have been plotted using gnuplot version 4.6 patchlevel 4. If not explicitly stated otherwise, all graphics have been created using the tikz package for LaTeX. Feynman diagrams have been drawn using the tikz-feynman package by Joshua Ellis.[2]

C.1 Numerical integration

There are many ways to approach the task of numerical integration. The simplest is the bar method, which approximates the integral of a function f over a given interval (a, b) by approximating the area under the function with rectangles of equal width and their height being the functions value at the center of each rectangle's base. This can be written as the equation

$$\int_a^b f(x)\mathrm{d}x \approx \sum_{i=1}^{N} f(x_i) \cdot \Delta x, \tag{C.1}$$

with $x_i = a + \frac{2i-1}{2N}(b-a)$ and $\Delta x = \frac{b-a}{N}$.
This method however is not very efficient as it only converges slowly for increasing

[1] Student's license
[2] jpellis.me/projects/tikz-feynman/

N. A faster method is the *Gauß-Legendre* method, where the function is no longer evaluated at equidistant points but instead is only evaluated at the specific set of points x_i which all have their own weight factor w_i, so that we get

$$\int_a^b f(x)\mathrm{d}x \approx \sum_{i=1}^{N} f(x_i) \cdot w_i. \tag{C.2}$$

With the correct choice of the abscissas and weights this method converges faster for smaller values of N. A subroutine to calculate appropriate values for the abscissas and weights can be found in [20].

C.2 Numerical differentiation

The procedure used to numerically find the derivative of a function follows a similar idea as the numerical integration. The idea is to start with the exact definition of the derivative

$$f'(x) := \lim_{\varepsilon \to 0} \frac{f(x+\varepsilon) - f(x)}{\varepsilon}. \tag{C.3}$$

Instead of going to the exact limit $\varepsilon \to 0$, we just plug in a small but non-zero value for ε. In general a smaller value for ε leads to a more precise result. If ε gets to small though, this method becomes unstable and might give wrong results. In this thesis $\varepsilon = 10^{-6}$ has been used for all derivatives, that have been done numerically.

C.3 Root finding methods

To find the zeros of the function $f(m) = \lambda(m) - 1$ the *false position method*, also called *regula falsi*, has been used. The method requires a continuous function f given in an interval $[x_1, x_2]$ with the condition $f(x_1) \cdot f(x_2) < 0$, assuring that a root can be found in the given interval. The idea behind this method is to approximate the function as linear in the interval. The linear approximation crosses the x-axis at a point $x_3 \in (x_1, x_2)$, which then replace one of the original points x_1 or x_2, depending on the sign of $f(x_3)$. This procedure is iterated over and over until a certain accuracy Δx is reached.

The false position method converges faster than most simpler methods, such as the bisection method. There are still methods that are faster, such as the secant method, but some do not converge at all for certain function, while the false position method always converges. An implementation of this method in C/C++ can be found in [20].

Bibliography

[1] C Patrignani, Particle Data Group, et al. Review of particle physics. *Chinese physics C*, 40(10):795, 2016.

[2] Michael Edward Peskin. *An introduction to quantum field theory*. Westview press, 1995.

[3] J. Gasser and H. Leutwyler. Quark masses. *Phys. Rep.*, 87:77, 1982.

[4] Gernot Eichmann, Hèlios Sanchis-Alepuz, Richard Williams, Reinhard Alkofer, and Christian S Fischer. Baryons as relativistic three-quark bound states. *Progress in Particle and Nuclear Physics*, 91:39, 2016.

[5] Michael R Pennington. Swimming with quarks. In *Journal of Physics: Conference Series*, volume 18, page 39. IOP Publishing, 2005.

[6] Christian S Fischer and Reinhard Alkofer. Nonperturbative propagators, running coupling, and the dynamical quark mass of landau gauge qcd. *Physical Review D*, 67(9):094020, 2003.

[7] Christian S Fischer. Infrared properties of qcd from dyson–schwinger equations. *Journal of Physics G: Nuclear and Particle Physics*, 32(8):R253, 2006.

[8] Gernot Eichmann. *Hadron properties from QCD bound-state equations*. PhD thesis, University of Graz, 2009.

[9] Pieter Maris and Craig D Roberts. π-and k-meson bethe-salpeter amplitudes. *Physical Review C*, 56(6):3369, 1997.

[10] Hannes LL Roberts, Lei Chang, Ian C Cloët, and Craig D Roberts. Masses of ground-and excited-state hadrons. *Few-body systems*, 51(1):1–25, 2011.

[11] Richard Williams. Bethe–salpeter studies of mesons beyond rainbow-ladder. In *EPJ Web of Conferences*, volume 3, page 03005. EDP Sciences, 2010.

[12] Pieter Maris, Craig D Roberts, and Peter C Tandy. Pion mass and decay constant. *Physics Letters B*, 420(3-4):267–273, 1998.

[13] HLL Roberts, A Bashir, LX Gutiérrez-Guerrero, CD Roberts, and DJ Wilson. π and ρ mesons, and their diquark partners, from a contact interaction. *Physical Review C*, 83(6):065206, 2011.

[14] VA Dzuba, VV Flambaum, and JK Webb. Space-time variation of physical constants and relativistic corrections in atoms. *Physical Review Letters*, 82(5):888, 1999.

[15] Nico Santowsky. Bound states of quarks and antiquarks in the bethe-salpeter formalism. Examination paper, Justus-Liebig-Universitaet, Giessen, 2017.

[16] Jonathan L Rosner, Sheldon Stone, and Ruth S Van de Water. Leptonic decays of charged pseudoscalar mesons-2015. *arXiv preprint arXiv:1509.02220*, 2015.

[17] Pieter Maris and Peter C Tandy. Qcd modeling of hadron physics. *Nuclear Physics B-Proceedings Supplements*, 161:136–152, 2006.

[18] YS Kim and Roger Zaoui. Lorentz contraction of the bethe-salpeter green's function. *Physical Review D*, 4(6):1764, 1971.

[19] Jeffrey Goldstone. Field theories with «superconductor» solutions. *Il Nuovo Cimento (1955-1965)*, 19(1):154–164, 1961.

[20] William H Press, Saul A Teukolsky, William T Vetterling, and Brian P Flannery. *Numerical recipes in C*, volume 2. Cambridge university press Cambridge, 1996.

Selbstständigkeitserklärung

Hiermit versichere ich, die vorgelegte Thesis selbstständig und ohne unerlaubte fremde Hilfe und nur mit den Hilfen angefertigt zu haben, die ich in der Thesis angegeben habe. Alle Textstellen, die wörtlich oder sinngemäß aus veröffentlichten Schriften entnommen sind, und alle Angaben die auf mündlichen Auskünften beruhen, sind als solche kenntlich gemacht. Bei den von mir durchgeführten und in der Thesis erwähnten Untersuchungen habe ich die Grundsätze guter wissenschaftlicher Praxis, wie sie in der ‚Satzung der Justus-Liebig-Universität zur Sicherung guter wissenschaftlicher Praxis' niedergelegt sind, eingehalten. Gemäß § 25 Abs. 6 der Allgemeinen Bestimmungen für modularisierte Studiengänge dulde ich eine Überprüfung der Thesis mittels Anti-Plagiatssoftware.

Gießen, den HIER DATUM EINFUEGEN

(Unterschrift)